ISSN: 2994-6433

Research Article

Journal of Sensor Networks and Data Communications

Bayesian Identifying One or Two Close Sources by Gaussian Estimates of Planar Location under Double Emission

Oleg I. Gerasimov*

Independent Researcher, Russian Federation

***Corresponding Author**
Oleg I. Gerasimov, Independent Researcher, Russian Federation.

Submitted: 2024, Dec 10; **Accepted:** 2025, Jan 17; **Published:** 2025, Jan 29

Citation: Gerasimov, O. I. (2025). Bayesian Identifying One or Two Close Sources by Gaussian Estimates of Planar Location under Double Emission. *J Sen Net Data Comm, 5*(1), 01-21.

Abstract

In case the separation for the parameters of interest appears below the resolution limit of the estimator, the ambiguity arises whether the two parameter estimates relate to one source emitted twice or to two close sources emitted once. The paper develops novel Bayes technique aimed to identify one/two closely spaced sources having a pair of Gaussian estimates of planar location as parameter. Prior probabilities of the one/two-sources hypotheses are available from the analysis of the physical characteristics of the emissions, assuming that they can be equally probable. The technique calculates minimal and maximal posterior probabilities of the hypotheses across all the positions at a given distance between them. When the minimal probability of one source is bigger than the maximal probability of two sources the decision is adopted in favor of one source and vice versa. Identification procedure is applied to distinguish two planar location estimates obtained for the users of basic station network by the time difference of arrival algorithm. The application gives an example of how the procedure revises the prior probabilities and can change thereby the initial preference with the distance between users.

Keywords: Separation to the Sources Location, Resolving Inequality, Probability of Resolving Inequality, Statistical Resolution Limit, Bayesian Inference, Identification Probability of One/Two-Sources

1. Introduction

Having two parameter estimates the problem whether one source emits twice or two sources at some separation between parameters below resolution limit emit once takes place in applications of the resolution theory. The existing approaches to identification parametrically close sources typically invoke probability of number of sources – either from subjective expert experience or Bayes inference, where such physical characteristics of a signal as spectrum, power and others are exploited. We come across the closest example of Bayes signal classification in radar, seismology and so on, when, having the probabilities of belonging of a signal to each class for each emission, it is not difficult to deduce probabilities of all possible numbers of sources for a given number of emissions using basic probability theorems [1,2]. In infrared optics, Bayesian logic is applied to obtain probability of number of neighboring screen images to overcome the smearing effect [3]. A similar problem arises in localization of blinking objects in microscopy where Bayesian framework is used to achieve probability of number of objects for the analysis below the diffraction limit [4-6]. We will refer to a solution that is able to provide the required probabilities of one and two sources as the prior solution (PS).

The resolution limit of the estimator is described by the Statistical Resolution Limit (*SRL*) defined as a minimal separation at which estimates are resolved correctly [7]. If the separation is less than *SRL*, then there will exist ambiguity about one or two sources. The concepts of *SRL* are primarily formulated in the detection theory and the estimation accuracy approach, [7,8-18]. Herein, we rely on the estimation accuracy utilizing the Cramer-Rao Bound **(CRB)** matrix-function of parameter, which under mild conditions represents a narrow lower bound on the covariance matrix of any unbiased estimator [19]. The equality to **CRB** is achieved in the class of efficient estimators to which we will address in the paper.

When resolving to the parameters p_1 and p_2 with separation Δp =*SRL*, $\Delta p = |p_2 - p_1|$, random separation between their estimates $|\Delta p'| = |p_2' - p_1'|$ centered at Δp satisfies the inequality $|\Delta p'| < \Delta p$, in which the separation estimate is smaller than the separation, with some probability. We will call this inequality the resolving inequality (*RI*) and the probability of *RI* abbreviate *PRI*. In scalar resolution criteria *SRL* is offered to be equal to standard deviation σ of the estimates difference for both decoupled and coupled estimates [15,7]. Thus, *PRI* for Gaussian noise $\Delta p'$ is $P\{|\Delta p'| < \sigma\}$ =0.9544:2=0.4772, i.e. it is close to 1/2. *SRL* is called to be consistent with *PRI* if *PRI* for that *SRL* occurs in the proximity of 1/2 (is equal to 1/2 up to the second decimal place). As we can see, *SRL*s from [15,7] are consistent.

With regard to vector case, separation should be expressed through a metric in parameter space, but *SRL* and *PRI* will clearly depend on variance of parameter component estimates and their covariance. The problem for multi-parameter estimates is considered in [16] by Korso, Boyer, Renaux and Marcos. Therein, *SRL*=*CRB*(δ), where separation δ between sets of parameters is the κ-norm distance (Minkowsky distance). Let us represent two scalar parameters $p^{(1)}, p^{(2)}$ in a vector form, $\boldsymbol{p} = \left[p^{(1)}, p^{(2)}\right]^T$ and denote estimates of vector $\boldsymbol{p}$ obtained from the decoupled emissions *1* and *2* as $\boldsymbol{p}_1'$, $\boldsymbol{p}_2'$ respectively. Then, the *RI* is written in metric of 1-norm (at $\kappa = 1$) of a difference vector $\Delta\boldsymbol{p}' = \boldsymbol{p}_1' - \boldsymbol{p}_2'$ as $\delta_{\kappa=1}(\Delta\boldsymbol{p}') = \|\Delta\boldsymbol{p}'\|_1 = \left|p_1'^{(1)} - p_2'^{(1)}\right| + \left|p_1'^{(2)} - p_2'^{(2)}\right| \le SRL$, $SRL^2 = \left(\sigma_1^{(1)}\right)^2 + \left(\sigma_1^{(2)}\right)^2 - 2\operatorname{cov}\left(p_1'^{(1)}, p_1'^{(2)}\right) + \left(\sigma_2^{(1)}\right)^2 + \left(\sigma_2^{(2)}\right)^2 - 2\operatorname{cov}\left(p_2'^{(1)}, p_2'^{(2)}\right)$. Variance and covariance are defined via underlying *CRB* functions obtained from applying change of variable formula to the extended measurement model of the estimator. This result formally extends scalar *SRL* on vector case, however *PRI*, i.e. the probability of $\|\Delta\boldsymbol{p}'\|_1 \le SRL$, could hardly be determined here in comparison with the scalar resolution criteria. Clark analyzing the resolution of estimator that produces vector decoupled Gaussian estimates offered weighted Euclidian metric of the distance between ellipsoidal confidence regions of probability 0.9 around each of the two parameters (really, Clark deals with the multiple vector parameter) [20]. The estimates are resolvable when the ellipsoids are disjoint. At the "resolution threshold" metric of the separation to the ellipsoids will be zero, and by this metric they will be tangent, but it is also not suitable to reach *PRI* unlike scalar case.

The paper considers the problem of identifying one/two sources by a pair of Gaussian decoupled estimates of planar location as parameter. The identifying is to perform in the domain of closely spaced sources where the covariance matrices of estimates are sufficiently approximated by a constant matrix, and thus *SRL* is also expected to be a constant. Discrimination positional estimates on the plane between blinking and close sources is relevant in mobile communication, molecular microscopy, astrometry and many other fields.

We construct novel Bayes technique with prior probabilities extracted from PS over two mutually exclusive events of Bayes sample space when the distance between sample estimates is either below or over *SRL*. The technique calculates the minimal and the maximal posterior probabilities of one and two sources across all the positions at a given distance between them. If the minimal probability of one source will be bigger than the maximal probability of two sources then we decide in favor of one source and vice versa. And thus, the probabilistic decision induced by PS can be revised with distance. To the best of our knowledge, no solution aimed to discriminate one source emitted twice and two close sources emitted once for a given pair of location estimates, which would be parameterized by the distance between hypothesized sources, has been considered previously.

When designing the event space, we need to have appropriate *SRL* concept for the planar decoupled estimates which would meet the following requirements: 1. *SRL* should be consistent with *PRI* when reducing to one-dimensional case and 2. the probability that the distance between estimates is smaller (bigger) than *SRL*, conditioned by the one/two-source hypotheses, should be computationally feasible. Clark's idea about the ellipsoidal confidence region is transformed herein to develop new *SRL* concept based on circular one of the high confidence probability to this end. Accordingly, *SRL* is said to be equal to the sum of the radii of confidence circles around each of the two parameters each of which contains parameter estimate with high (near to unity) probability, i.e. the circles at the *separation*=*SRL* are tangent. As shown in the study, *PRI* for proposed *SRL* reaches the proximity of 1/2 as long as the planar concentration ellipsoid (CE) (the term is borrowed from [21]) of estimates difference is shrinking along the minor axis and by that degenerating towards a scalar case. The computation of the probability required is feasible for a given difference between the parameters and the covariance matrices of each estimate. If the circles around location sample estimates intersect the distance between them occurs below *SRL*, otherwise, when they are disjoint – over *SRL* in Bayes event space.

The technique's work is illustrated in the example of distinguishing two positional estimates between one and two close each other users of the time difference of arrival (TDOA) basic stations (BS)s network. The signals there are classified to derive the initial probabilities of one and two users. The solution must answer the following question: does one user emit twice or do two users at some distance between them emit once. The technique implementation is based on the radius of the high confidence circle obtained in the paper for the confidence probability 0.99. This radius will subsequently be denoted as *R99*.

The rest of the paper is organized as follows. The problem is described in Section 2. New concept of *SRL* is founded in Section 3. Section 4 contains the design of Bayesian identification technique. The algorithm for estimation of *R99* is presented in Section 5. Proposed technique as applied in TDOA BSs network is quantitatively studied in Section 6. Section 7 briefly draws the summary of the paper.

2. Statement of the Problem

During two consecutive time intervals T^{I} and T^{II}: $T^{I}\bigcap T^{II}=\varnothing$, $t^{I}\in T^{I}$, $t^{II}\in T^{II}$, L signals from emission *I* and *L* signals from emission *II* are received. The k - th signal depends upon vector parameter $\boldsymbol{q}$, $\boldsymbol{q}\in\{\boldsymbol{q}^{I},\boldsymbol{q}^{II}\}$, gathering physical characteristics of the emissions, and m - dimensional measurement parameter $\boldsymbol{p}_k(\boldsymbol{\varphi})$ which is a known smooth function of a two-dimensional unknown vector of the source location, $\boldsymbol{\varphi}\in\{\boldsymbol{\varphi}^{I},\boldsymbol{\varphi}^{II}\}$:

$$\begin{aligned}
&\boldsymbol{V}(t^{I})=\left[\boldsymbol{v}^{T}\left(t^{I};\boldsymbol{q}^{I},\boldsymbol{p}_1(\boldsymbol{\varphi}^{I})\right),\ldots,\boldsymbol{v}^{T}\left(t^{I};\boldsymbol{q}^{I},\boldsymbol{p}_L(\boldsymbol{\varphi}^{I})\right)\right]^{T},\\
&\boldsymbol{V}(t^{II})=\left[\boldsymbol{v}^{T}\left(t^{II};\boldsymbol{q}^{II},\boldsymbol{p}_1(\boldsymbol{\varphi}^{II})\right),\ldots,\boldsymbol{v}^{T}\left(t^{II};\boldsymbol{q}^{II},\boldsymbol{p}_L(\boldsymbol{\varphi}^{II})\right)\right]^{T},\\
&\boldsymbol{v}\left(t;\boldsymbol{q},\boldsymbol{p}_k(\boldsymbol{\varphi})\right)=\boldsymbol{g}\left(t;\boldsymbol{q},\boldsymbol{p}_k(\boldsymbol{\varphi})\right)+\boldsymbol{n}_k(t),\ t\in\{T^{I},T^{II}\},
\end{aligned}\tag{1}$$

where $\boldsymbol{g}(t;\boldsymbol{q},\boldsymbol{p}_k)$ is a waveform vector-function of time and parameters $\boldsymbol{q}$, $\boldsymbol{p}_k$; $\boldsymbol{n}_k(t)$ is unbiased Gaussian noise with $E\left\{\boldsymbol{n}_i(t^{I})\boldsymbol{n}_j^{T}(t^{II})\right\}=\boldsymbol{0}$ for the all $i,j\le L$, $E\{\cdot\}$ denotes mathematical expectation operator

Unbiased estimator $\Im_p$ establishes the inverse relation between signals (1) and measurement vectors $\boldsymbol{p}'$ and $\boldsymbol{p}''$, $\tilde{\boldsymbol{p}}=\Im_p\{\boldsymbol{V}(t)\}$, $\tilde{\boldsymbol{p}}\in\{\boldsymbol{p}',\boldsymbol{p}''\}$, related to emissions *I* and *II*:

$$\begin{aligned}
&\tilde{\boldsymbol{p}}=\boldsymbol{p}(\boldsymbol{\varphi})+\boldsymbol{\upsilon},\ \boldsymbol{p}(\boldsymbol{\varphi})=\left[\boldsymbol{p}_1^{T}(\boldsymbol{\varphi}),\ldots,\boldsymbol{p}_{L_p}^{T}(\boldsymbol{\varphi})\right]^{T},\ L_p\le L,\\
&\boldsymbol{\upsilon}\in\{\boldsymbol{\upsilon}',\boldsymbol{\upsilon}''\},\ \boldsymbol{\upsilon}'=\left[\boldsymbol{\upsilon}_1'^{T},\ldots,\boldsymbol{\upsilon}_{L_p}'^{T}\right]^{T},\ \boldsymbol{\upsilon}''=\left[\boldsymbol{\upsilon}_1''^{T},\ldots,\boldsymbol{\upsilon}_{L_p}''^{T}\right]^{T},\\
&\boldsymbol{\upsilon}_k=\left[\upsilon_{k1},\ldots\upsilon_{km}\right]^{T},\ k=\overline{1,L_p},
\end{aligned}\tag{2}$$

where $\boldsymbol{\upsilon}'$ and $\boldsymbol{\upsilon}''$ are the measurement errors corresponding to the emissions *I* and *II* with $E\left\{\boldsymbol{\upsilon}'\boldsymbol{\upsilon}''^{T}\right\}=\boldsymbol{0}$, i.e. $\boldsymbol{p}'$ and $\boldsymbol{p}''$ are decoupled. Unbiased estimator $\Im_\varphi$ uses measurements (2) to produce estimates $\boldsymbol{\varphi}'$ and $\boldsymbol{\varphi}''$ over the emissions *I* and *II*: $\tilde{\boldsymbol{\varphi}}=\Im_\varphi(\tilde{\boldsymbol{p}})$, $\tilde{\boldsymbol{\varphi}}\in\{\boldsymbol{\varphi}',\boldsymbol{\varphi}''\}$, $\tilde{\boldsymbol{\varphi}}=\boldsymbol{\varphi}+\boldsymbol{\varsigma}$, $\boldsymbol{\varsigma}\in\{\Delta\boldsymbol{\varphi}',\Delta\boldsymbol{\varphi}''\}$, where $\Delta\boldsymbol{\varphi}'$ and $\Delta\boldsymbol{\varphi}''$ are the corresponding errors, which are also decoupled.

We consider (***a***) "regular enough" algorithms $\Im_p$ and $\Im_\varphi$ such that $\tilde{\boldsymbol{p}}$ and $\tilde{\boldsymbol{\varphi}}$ are both normally distributed with the covariance matrix $\boldsymbol{\Pi}$ of the estimate $\tilde{\boldsymbol{p}}$ and an unknown one $\boldsymbol{\Phi}(\boldsymbol{\varphi})$ of the estimate $\tilde{\boldsymbol{\varphi}}$ [22]. The estimators $\Im_p$ and $\Im_\varphi$ are assumed (***b***) to be efficient, hence $\boldsymbol{\Phi}$ is calculated as **CRB** by use of the Fisher Information Matrix $\mathbf{FIM}(\boldsymbol{\varphi})$: $\boldsymbol{\Phi}(\boldsymbol{\varphi})=\mathbf{CRB}(\boldsymbol{\varphi})=\mathbf{FIM}^{-1}(\boldsymbol{\varphi})$. For Gaussian noise, $\mathbf{FIM}(\boldsymbol{\varphi})=\left[\dfrac{\partial\boldsymbol{p}(\boldsymbol{\varphi})}{\partial\boldsymbol{\varphi}}\right]^{T}\boldsymbol{\Pi}^{-1}\left[\dfrac{\partial\boldsymbol{p}(\boldsymbol{\varphi})}{\partial\boldsymbol{\varphi}}\right]$.

The hypotheses H_α and H_β serve to specify the sources of emissions: the hypothesis H_α means that one source at $\boldsymbol{\varphi}_1=\boldsymbol{\varphi}^{I}=\boldsymbol{\varphi}^{II}$ with $\boldsymbol{q}_1=\boldsymbol{q}^{I}=\boldsymbol{q}^{II}$ emits twice, the hypothesis H_β – that each of the two sources at $\boldsymbol{\varphi}_1=\boldsymbol{\varphi}^{I}$ and $\boldsymbol{\varphi}_2=\boldsymbol{\varphi}^{II}$ with $\boldsymbol{q}_1=\boldsymbol{q}^{I}$ and $\boldsymbol{q}_2=\boldsymbol{q}^{II}$ emit once. The probabilities $P\{\mathrm{H}_\alpha\}$ and $P\{\mathrm{H}_\beta\}$ of the hypotheses come from a preceding step of data processing where parameter $\boldsymbol{q}$ can be involved.

We define the circles $\boldsymbol{S}_1 = \{\boldsymbol{\varphi} : \|\boldsymbol{\varphi} - \boldsymbol{\varphi}_1\| \le R_1\}$ and $\boldsymbol{S}_2 = \{\boldsymbol{\varphi} : \|\boldsymbol{\varphi} - \boldsymbol{\varphi}_2\| \le R_2\}$, $\|\bullet\|$ denotes Euclidian norm, with radii R_1 and R_2 where estimates $\boldsymbol{\varphi}'$ and $\boldsymbol{\varphi}''$ fall with high probability P_S: $\tilde{\boldsymbol{\varphi}} \in \boldsymbol{S}_1$ for H_α and $\boldsymbol{\varphi}' \in \boldsymbol{S}_1$, $\boldsymbol{\varphi}'' \in \boldsymbol{S}_2$ for H_β. It is assumed (c) that sample covariance matrices inside $\boldsymbol{S}_1$ and $\boldsymbol{S}_2$ coincide with $\boldsymbol{\Phi}(\boldsymbol{\varphi}_1)$ and $\boldsymbol{\Phi}(\boldsymbol{\varphi}_2)$ with high accuracy. Due to negligible probability $1 - P_S^2$ of outliers beyond circles we will treat estimates $\boldsymbol{\varphi}'$ and $\boldsymbol{\varphi}''$ so that as if $\boldsymbol{\varphi}'$, $\boldsymbol{\varphi}'' \in \boldsymbol{S}_1$ or $\boldsymbol{\varphi}' \in \boldsymbol{S}_1$, $\boldsymbol{\varphi}'' \in \boldsymbol{S}_2$.

The identifying is performed in the domain $\boldsymbol{S}_0$ centered at $\boldsymbol{\varphi}_1$ where covariance matrices $\boldsymbol{\Phi}(\boldsymbol{\varphi}_2)$ are assumed (***d***) to be sufficiently approximated by a constant matrix. It follows the assumption (***d***) that the radius $R_2 = R_2(\boldsymbol{\varphi}_2)$ is also approximated in $\boldsymbol{S}_0$ by a constant. Let us define domain $\boldsymbol{S}_0$ as $\boldsymbol{S}_0 = \{\boldsymbol{\varphi}_2 : \|\boldsymbol{\varphi}_2 - \boldsymbol{\varphi}_1\| \le R_S + \delta R_S\}$, $R_S = R_1 + R_2$, $\delta R_S < R_S$, and specify it as the domain of closely spaced sources.

The goal is to find probabilistic decision of the problem whether one source at position $\boldsymbol{\varphi}_1$ emits twice or two sources at positions $\boldsymbol{\varphi}_1$ and $\boldsymbol{\varphi}_2$ emit once for a given separation $r = \|\boldsymbol{\varphi}_1 - \boldsymbol{\varphi}_2\|$ with the sample estimates $\hat{\boldsymbol{\varphi}}'$ and $\hat{\boldsymbol{\varphi}}''$ of the random variables $\boldsymbol{\varphi}'$ and $\boldsymbol{\varphi}''$ on the conditions (***a***), (***b***), (***c***) and (***d***).

3. The Concept of *SRL* Based on High Confidence Circle

In the frame of this Section, variables $\boldsymbol{\varphi}'$ and $\boldsymbol{\varphi}''$ are considered as just the Gaussian two-dimensional estimates, not necessarily of location coordinate, with $E\{\boldsymbol{\varphi}'\} = \boldsymbol{\varphi}_1$ and $E\{\boldsymbol{\varphi}''\} = \boldsymbol{\varphi}_2$. The difference between the estimates $\boldsymbol{\psi} = \boldsymbol{\varphi}'' - \boldsymbol{\varphi}'$ is Gaussian with a mean $\bar{\boldsymbol{\psi}} = \boldsymbol{\varphi}_2 - \boldsymbol{\varphi}_1$ and covariance matrix $\mathbf{W}_\psi = \boldsymbol{\Phi}(\boldsymbol{\varphi}_1) + \boldsymbol{\Phi}(\boldsymbol{\varphi}_2)$ with eigenvalues $l_1 > l_2 > 0$. We propose the concept of *SRL* based on the circles $\boldsymbol{S}_1$ and $\boldsymbol{S}_2$ being tangent. This happens at the separation $\|\boldsymbol{\varphi}_1 - \boldsymbol{\varphi}_2\| = R_S$, which is accepted to be *SRL*. *PRI* of that resolution criterion, $PRI_S = P\{(\|\boldsymbol{\psi}\| \,|\, \|\bar{\boldsymbol{\psi}}\| = R_S) \le R_S\}$, is defined by the following Theorem.

Theorem.

$$0.5P_S^2 - \frac{1}{\pi}\left[\frac{\pi}{2} + arctg\left(\sqrt{\frac{l_1}{l_2}}tg\frac{2\pi}{3}\right)\right] < PRI_S < 0.5P_S^2.$$

Proof of Theorem.

1. The region $\boldsymbol{\Sigma}$ encompassing $\bar{\boldsymbol{\psi}}$, where $\boldsymbol{\psi}$ falls with probability P_S^2 (we treat estimates of interest as $\boldsymbol{\varphi}' \in \boldsymbol{S}_1$, $\boldsymbol{\varphi}'' \in \boldsymbol{S}_2$, see Section 2), is represented in polar coordinates (r'', ϑ''), (r', ϑ') as $\boldsymbol{\Sigma} = \left\{\bar{\boldsymbol{\psi}} + \begin{bmatrix} r''\cos\vartheta'' - r'\cos\vartheta' \\ r''\sin\vartheta'' - r'\sin\vartheta' \end{bmatrix}\right\}$, $r'' \in (0, R_2]$, $r' \in (0, R_1]$ and $\vartheta'' \in [0, 2\pi]$, $\vartheta' \in [0, 2\pi]$. The squared distance from $\bar{\boldsymbol{\psi}}$ to any point of $\boldsymbol{\Sigma}$ is $(r'')^2 + (r')^2 - 2r''r'\cos(\vartheta'' - \vartheta')$ maximum of which is achieved at $r'' = R_2$, $r' = R_1$, $\vartheta'' - \vartheta' = \pi$ and is equal to $(R_1 + R_2)^2$. Consequently, $\boldsymbol{\Sigma}$ is a circle centered at $\bar{\boldsymbol{\psi}}$ with radius R_S bounded by the circumference $\boldsymbol{\Sigma}_C$ including the origin.

2. The region $\boldsymbol{\Xi}$ of desired probability is formed by the intersection of the circles $\boldsymbol{\Sigma}$ and $\boldsymbol{\Lambda} = \{\boldsymbol{\psi} : \|\boldsymbol{\psi}\| \le R_S\}$ (due to realizations of $\boldsymbol{\psi}$ is considered to belong to $\boldsymbol{\Sigma}$), see Fig. 1a. Straight line L connecting the intersection points of circumferences $\boldsymbol{\Sigma}_C$ and $\boldsymbol{\Lambda}_C$ is collinear in virtue of symmetry to the tangent T to $\boldsymbol{\Lambda}_C$ at the point $\bar{\boldsymbol{\psi}}$. It divides the line from origin to $\bar{\boldsymbol{\psi}}$ on two identical segments, hence the angle θ is equal to $\pi/6$, see Fig. 1a again. We successively move $\bar{\boldsymbol{\psi}}$ to the origin and rotate

coordinates to write probability integral over $\varXi$ in terms of spectrum of $\mathbf{W}_\psi$. Changing to polar coordinates (s, ϕ) one gets

$$P\{\boldsymbol{\psi} \in \varXi\} = \frac{1}{2\pi\sqrt{l_1 l_2}} \int_{\pi/2+\pi/6}^{3\pi/2-\pi/6} d\phi \int_0^{s(\phi)} s \exp\left[-\frac{s^2 g(\phi; l_1, l_2)}{2}\right] \mathrm{d}s, \tag{3}$$

where $g(\phi;l_1,l_2) \equiv (l_1^{-1}\cos^2\phi + l_2^{-1}\sin^2\phi)$. The ordinate divides Σ into two semicircles Σ_{left} and Σ_{right}, but two identical regions Σ_u and Σ_d associated with $\pi/6$ complement $\varXi$ to semicircle Σ_{left}, Fig. 1b. From the symmetry of probability density in integral (3) with respect to the angle ϕ one has $P\{\boldsymbol{\psi} \in \boldsymbol{\Sigma}_{left}\} = P\{\boldsymbol{\psi} \in \boldsymbol{\Sigma}_{right}\} = 0.5P_S^2$ and $P\{\boldsymbol{\psi} \in \boldsymbol{\Sigma}_u\} = P\{\boldsymbol{\psi} \in \boldsymbol{\Sigma}_d\}$.

3. We represent probability (3) as

$$P\{\boldsymbol{\psi} \in \varXi\} = 0.5P_S^2 - \frac{1}{\pi\sqrt{l_1 l_2}} \int_{\pi/2}^{2\pi/3} \mathrm{d}\phi \int_0^{s(\phi)} s \exp\left[-\frac{s^2 g(\phi; l_1, l_2)}{2}\right] \mathrm{d}s, \tag{4}$$

where $s(\phi) = 2R_S \sin(\phi - \pi/2) = -2R_S \cos\phi$, see Fig 1b again.

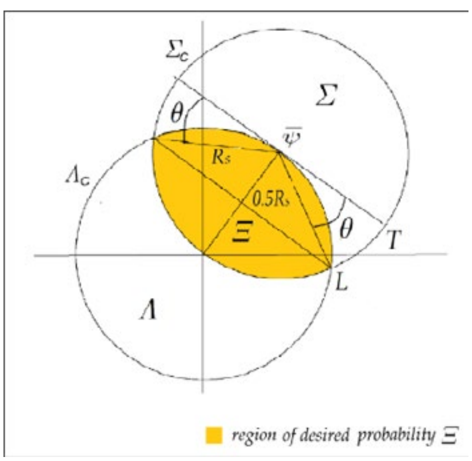

(a)

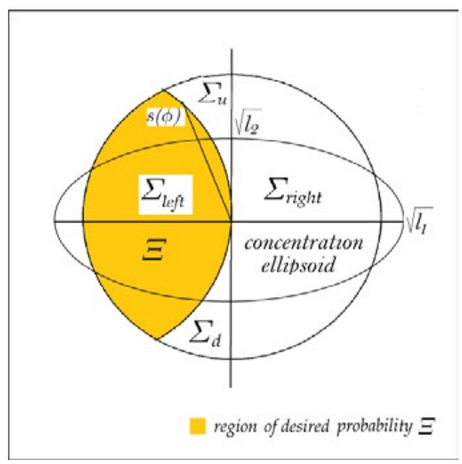

(b)

Figure 1: The Region $\varXi$ of Desired Probability: (a) In Initial Coordinates, (b) In Transformed Coordinates.

Performing the integral in (4) over variable s leads to the integral over ϕ in equality (4):

$$P\{\boldsymbol{\psi} \in \varXi\} = 0.5P_S^2 - \frac{1}{\pi\sqrt{l_1 l_2}} \int_{\pi/2}^{2\pi/3} \frac{\{1 - \exp[-2R_S^2 g(\phi; l_1, l_2)\cos^2\phi]\}\mathrm{d}\phi}{g(\phi; l_1, l_2)}.$$

We maximize it over ϕ to evaluate $P\{\psi \in \varXi\}$ from below:

$$P\{\boldsymbol{\psi} \in \varXi\} > 0.5P_S^2 - \max_\phi\{1 - \exp[-2R_S^2 g(\phi; l_1, l_2)\cos^2\phi]\} \frac{1}{\pi\sqrt{l_1 l_2}} \int_{\pi/2}^{2\pi/3} \frac{\mathrm{d}\phi}{g(\phi; l_1, l_2)}. \tag{5}$$

It can be easily verified that the derivative of the exponential function from (5) is non-positive, thus required maximum is achieved at $\phi=2\pi/3$ and is equal to $\left(1-\mathrm{e}^{-\frac{R_S^2}{2}\left(\frac{1}{4l_1}+\frac{3}{4l_2}\right)}\right)$. We substitute l_1 with l_2 in exponent and perform integration in (5), after that come to inequality [23]:

$$P\{\boldsymbol{\psi}\in\boldsymbol{\Xi}\}>0.5P_S^2-\left(1-\mathrm{e}^{-\frac{R_S^2}{2l_2}}\right)\frac{1}{\pi}\left[\frac{\pi}{2}+arctg\left(\bar{e}tg\frac{2\pi}{3}\right)\right],$$

where $\bar{e}=\sqrt{l_1/l_2}$. Factor $\left(1-\mathrm{e}^{-\frac{R_S^2}{2l_2}}\right)$ is the probability that realizations of $\boldsymbol{\psi}$ will be in CE centered at origin with principal semi-minor axis R_S and semi-major axis $\bar{e}R_S$ [21]. Region $\boldsymbol{\Sigma}$ which contains $\boldsymbol{\psi}$ with probability P_S^2 is the circle inscribed in the CE, thus confidence probability of the latter will be closer to unity than P_S^2. And if so, we substitute it with unity and end the Proof.

Theorem ensures $PRI_S<0.5P_S^2$, while low bound of PRI_S depends on spectral characteristic $\bar{e}$. Function $1/2+\pi^{-1}arctg\left[\bar{e}tg(2\pi/3)\right]$ tied with the magnitude of integral $P\{\boldsymbol{\psi}\in\boldsymbol{\Sigma}_u\}$ is monotonically decreasing with the growth of $\bar{e}$: it approaches zero at $\bar{e}\to\infty$ providing $PRI_S\to 0.4905$ for $P_S=0.99$. In that asymptotic behavior of integral $P\{\boldsymbol{\psi}\in\boldsymbol{\Sigma}_u\}$ CE is shrinking along the minor semi-axis $\sqrt{l_2}$ and elongating on the major semi-axis $\sqrt{l_1}$, hence the probability mass (the term is borrowed from [20]) shifts to the one-dimensional estimate, and $P\{\boldsymbol{\psi}\in\boldsymbol{\Sigma}_u\}\to 0$ because of that. The consistency of *SRL* manifests itself in the widest range of covariance matrix spectrum: let's say, $\bar{e}>10$ then we get $PRI_S>0.4721$ and can declare that PRI_S occurs in a proximity of $1/2$. With the rest of the spectrum, at $\bar{e}\to 1$, when $l_1\to l_2$, this function approaches its maximum $1/6$, providing $PRI_S>0.4905-0.1667=0.3238$. CE is here transforming into the circle with radius $l=l_1=l_2$ and $g(\phi;l_1,l_2)=l^{-1}$; thus integral $2P\{\boldsymbol{\psi}\in\boldsymbol{\Sigma}_u\}=1/6-\pi^{-1}\int_{\pi/2}^{2\pi/3}\mathrm{e}^{-\frac{2R_S^2}{l}\cos^2\phi}\mathrm{d}\phi$ will be just under $1/6$.

Probability $P\left\{\left(\|\boldsymbol{\psi}\|^2\middle|\bar{\boldsymbol{\psi}},\mathbf{W}_\psi\right)\le R_S^2\right\}=1-P\left\{\left(\|\boldsymbol{\psi}\|^2\middle|\bar{\boldsymbol{\psi}},\mathbf{W}_\psi\right)>R_S^2\right\}$ is referred to a distribution of a quadratic form $\boldsymbol{\psi}^T\mathbf{A}\boldsymbol{\psi}$, where $\boldsymbol{\psi}$ is non-central Gaussian vector with a mean $\bar{\boldsymbol{\psi}}$ and covariance matrix $\mathbf{W}_\psi$, $\mathbf{A}$ is a symmetric and nonnegative definite matrix. We obtain the desired distribution by equating $\mathbf{A}$ to the identity matrix. Although its mathematical structure is complicated, modern computer resources allow to implement supporting functions precisely [24].

Remark 1. The probability is computed in [24] over the entire circle Λ (or outside it), not only over intersection of Λ and $\boldsymbol{\Sigma}$ centered at some $\bar{\boldsymbol{\psi}}$ with $\|\bar{\boldsymbol{\psi}}\|=r$. However, this additional contribution is negligible being less than $1-P_S^2$.

4. Bayesian Identification Technique

The sample analogues $\mathbf{\Phi}\left(\hat{\boldsymbol{\varphi}}'\right)$ and $\mathbf{\Phi}\left(\hat{\boldsymbol{\varphi}}''\right)$ of one or two true covariance matrices are employed to achieve the approximation $\bar{R}_S$ of R_S as $\bar{R}_S = R'_S + R''_S$ where estimates R'_S, R''_S approximate R_1 twice or R_1, R_2 once. The sample covariance matrix of random variable ψ is $\hat{\mathbf{W}}_\psi = \mathbf{\Phi}\left(\hat{\boldsymbol{\varphi}}'\right) + \mathbf{\Phi}\left(\hat{\boldsymbol{\varphi}}''\right)$. The event space C is defined to consist of two events, when the confidence circles encompassing sample estimates $\hat{\boldsymbol{\varphi}}'$ and $\hat{\boldsymbol{\varphi}}''$ intersect: $\left\|\hat{\boldsymbol{\varphi}}'' - \hat{\boldsymbol{\varphi}}'\right\| \le \bar{R}_S$ at $\mathrm{C} = \mathrm{C}_1$ or do not intersect: $\left\|\hat{\boldsymbol{\varphi}}'' - \hat{\boldsymbol{\varphi}}'\right\| > \bar{R}_S$ at $\mathrm{C} = \mathrm{C}_2$. Conditioned by the hypotheses H_α and H_β probabilities of the events C_1 and C_2 are $P\{\mathrm{C}_1|\mathrm{H}_\alpha\} = P\left\{\left(\|\boldsymbol{\psi}\|^2 \middle| \bar{\boldsymbol{\psi}} = \mathbf{0}\right) \le \bar{R}_S^2\right\}$ and $P\{\mathrm{C}_1|\mathrm{H}_\beta\} = P\left\{\left(\|\boldsymbol{\psi}\|^2 \middle| \bar{\boldsymbol{\psi}} \ne \mathbf{0}\right) \le \bar{R}_S^2\right\}$, $P\{\mathrm{C}_2|\mathrm{H}_\alpha\} = P\left\{\left(\|\boldsymbol{\psi}\|^2 \middle| \bar{\boldsymbol{\psi}} = \mathbf{0}\right) > \bar{R}_S^2\right\}$ and $P\{\mathrm{C}_2|\mathrm{H}_\beta\} = P\left\{\left(\|\boldsymbol{\psi}\|^2 \middle| \bar{\boldsymbol{\psi}} \ne \mathbf{0}\right) > \bar{R}_S^2\right\}$.

The probability $P\{\mathrm{C}_1|\mathrm{H}_\alpha\}$ is near to unity hence $P\{\mathrm{C}_2|\mathrm{H}_\alpha\} = 1 - P\{\mathrm{C}_1|\mathrm{H}_\alpha\}$ is near to zero. The probability $P\{\mathrm{C}_1|\mathrm{H}_\beta\}$ decreases asymptotically with the rise of $\|\bar{\psi}\|$ consequently the probability $P\{\mathrm{C}_2|\mathrm{H}_\beta\} = 1 - P\{\mathrm{C}_1|\mathrm{H}_\beta\}$ asymptotically increases. $P\{\mathrm{C}_1|\mathrm{H}_\beta\}$ is smaller than $P\{\mathrm{C}_1|\mathrm{H}_\alpha\}$ approaching it from below at $\|\bar{\psi}\| \to 0$, while $P\{\mathrm{C}_2|\mathrm{H}_\beta\}$ is bigger than $P\{\mathrm{C}_2|\mathrm{H}_\alpha\}$ approaching it from above at $\|\bar{\psi}\| \to 0$. $P\{\mathrm{C}|\mathrm{H}_\beta\}$ depends on covariance matrix $\hat{\mathbf{W}}_\psi$ and an unknown mean $\bar{\psi}$; $P\{\mathrm{C}|\mathrm{H}_\alpha\}$ depends only on $\hat{\mathbf{W}}_\psi$.

We develop Bayesian scheme with the minimal and maximal posterior probabilities of hypotheses H_α and H_β to be determined on the circumference $\mathbb{C}_r = \{\bar{\psi} : \|\bar{\psi}\| = r\}$ where equidistant from φ_1 positions φ_2 run, both at $r \le \bar{R}_S$ and at $r > \bar{R}_S$, see Fig. 2.

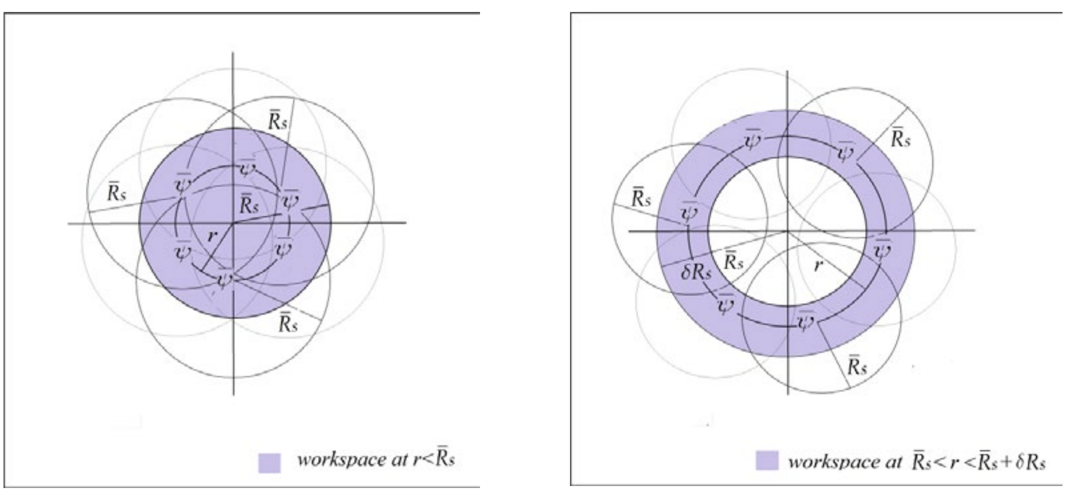

(a) (b)

Figure 2: The Workspace of the Bayesian Technique: (a) Below and (b) Over Resolution Limit $\bar{R}_S$. The Circles are to Depict the Region Σ where Estimates Fall for the Each $\bar{\psi} \in \mathbb{C}_r$.

Prior probabilities of the scheme come from PS. Let us denote minimal and maximal on $\mathbb{C}_r$ posterior probabilities of H_β as $P^{\beta}_{\min}(\mathrm{C};r) = \min\left(P\left\{\mathrm{H}_\beta|\mathrm{C}\right\}, \bar{\boldsymbol{\psi}} \in \mathbb{C}_r\right)$ and $P^{\beta}_{\max}(\mathrm{C};r) = \max\left(P\left\{\mathrm{H}_\beta|\mathrm{C}\right\}, \bar{\boldsymbol{\psi}} \in \mathbb{C}_r\right)$. By the binary Bayesian theorem,

$$P^{\beta}_{\max}(\mathrm{C};r) = \frac{P\left\{\mathrm{H}_\beta\right\} P^{+}_{\mathrm{C}}(r)}{P\left\{\mathrm{H}_\alpha\right\} P\left\{\mathrm{C}|\mathrm{H}_\alpha\right\} + P\left\{\mathrm{H}_\beta\right\} P^{+}_{\mathrm{C}}(r)}, \tag{6}$$

$$P^{\beta}_{\min}(\mathrm{C};r) = \frac{P\left\{\mathrm{H}_\beta\right\} P^{-}_{\mathrm{C}}(r)}{P\left\{\mathrm{H}_\alpha\right\} P\left\{\mathrm{C}|\mathrm{H}_\alpha\right\} + P\left\{\mathrm{H}_\beta\right\} P^{-}_{\mathrm{C}}(r)}, \tag{7}$$

where $P^{-}_{\mathrm{C}}(r) = \min\left(P\left\{\mathrm{C}|\mathrm{H}_\beta\right\}, \bar{\boldsymbol{\psi}} \in \mathbb{C}_r\right)$ and $P^{+}_{\mathrm{C}}(r) = \max\left(P\left\{\mathrm{C}|\mathrm{H}_\beta\right\}, \bar{\boldsymbol{\psi}} \in \mathbb{C}_r\right)$ are conditioned by H_β extreme probabilities. Minimal $P^{\alpha}_{\min}(\mathrm{C};r)$ and maximal $P^{\alpha}_{\max}(\mathrm{C};r)$ on $\mathbb{C}_r$ aposterior of H_α are

$$P^{\alpha}_{\min}(\mathrm{C};r) = \frac{P\left\{\mathrm{H}_\alpha\right\} P\left\{\mathrm{C}|\mathrm{H}_\alpha\right\}}{P\left\{\mathrm{H}_\alpha\right\} P\left\{\mathrm{C}|\mathrm{H}_\alpha\right\} + P\left\{\mathrm{H}_\beta\right\} P^{+}_{\mathrm{C}}(r)}, \tag{8}$$

$$P^{\alpha}_{\max}(\mathrm{C};r) = \frac{P\left\{\mathrm{H}_\alpha\right\} P\left\{\mathrm{C}|\mathrm{H}_\alpha\right\}}{P\left\{\mathrm{H}_\alpha\right\} P\left\{\mathrm{C}|\mathrm{H}_\alpha\right\} + P\left\{\mathrm{H}_\beta\right\} P^{-}_{\mathrm{C}}(r)}. \tag{9}$$

Extreme probabilities (6–9) are the monotonic functions along r due to $P^{-}_{\mathrm{C}_1}(r)$ and $P^{+}_{\mathrm{C}_1}(r)$ decrease monotonically with the rise of r, accordingly functions $P^{-}_{\mathrm{C}_2}(r) = 1 - P^{+}_{\mathrm{C}_1}(r)$ and $P^{+}_{\mathrm{C}_2}(r) = 1 - P^{-}_{\mathrm{C}_1}(r)$ monotonically increase. This stems from the following Lemma.

Lemma. $P^{-}_{\mathrm{C}_1}(r) > P^{-}_{\mathrm{C}_1}(r')$, $P^{+}_{\mathrm{C}_1}(r) > P^{+}_{\mathrm{C}_1}(r')$ at $r < r'$.

Proof of Lemma. For some pair of vectors $\bar{\boldsymbol{\psi}}_r = r\bar{\boldsymbol{\psi}}_1$ and $\bar{\boldsymbol{\psi}}_{r'} = r'\bar{\boldsymbol{\psi}}_1$, $\bar{\boldsymbol{\psi}}_1 \in \mathbb{C}_1$ one has variables ψ_r and $\psi_{r'}$ with means $\bar{\boldsymbol{\psi}}_r \in \mathbb{C}_r$ and $\bar{\boldsymbol{\psi}}_{r'} \in \mathbb{C}_{r'}$. Then, $\|\boldsymbol{\psi}_r\|^2 = r^2 + r2\bar{\boldsymbol{\psi}}_1^T \Delta\boldsymbol{\psi} + \|\Delta\boldsymbol{\psi}\|^2$, $\|\boldsymbol{\psi}_{r'}\|^2 = r'^2 + r'2\bar{\boldsymbol{\psi}}_1^T \Delta\boldsymbol{\psi} + \|\Delta\boldsymbol{\psi}\|^2$. Variances of $r'2\bar{\boldsymbol{\psi}}_1^T \Delta\boldsymbol{\psi}$ and $r2\bar{\boldsymbol{\psi}}_1^T \Delta\boldsymbol{\psi}$ are variance of $2\bar{\boldsymbol{\psi}}_1^T \Delta\boldsymbol{\psi}$ multiplied by the factors r'^2 and r^2 correspondently, and from the properties of normal distribution $P\left\{\left(r^2 + r2\bar{\boldsymbol{\psi}}_1^T \Delta\boldsymbol{\psi}\right) \le \bar{R}_S^2\right\} > P\left\{\left(r'^2 + r'2\bar{\boldsymbol{\psi}}_1^T \Delta\boldsymbol{\psi}\right) \le \bar{R}_S^2\right\}$. So, $P\left\{\|\boldsymbol{\psi}_r\|^2 \le \bar{R}_S^2\right\} > P\left\{\|\boldsymbol{\psi}_{r'}\|^2 \le \bar{R}_S^2\right\}$ that completes the Proof.

Corollary. $P^{\beta}_{\min}(\mathrm{C}_1;r)$, $P^{\beta}_{\max}(\mathrm{C}_1;r)$, $P^{\alpha}_{\min}(\mathrm{C}_2;r)$, $P^{\alpha}_{\max}(\mathrm{C}_2;r)$ decrease with r monotonically; $P^{\beta}_{\min}(\mathrm{C}_2;r)$, $P^{\beta}_{\max}(\mathrm{C}_2;r)$, $P^{\alpha}_{\min}(\mathrm{C}_1;r)$, $P^{\alpha}_{\max}(\mathrm{C}_1;r)$ – monotonically increase.

The preference of a hypothesis is achievable when $P^{\alpha}_{\min}(\mathrm{C};r) > P^{\beta}_{\max}(\mathrm{C};r)$ or $P^{\beta}_{\min}(\mathrm{C};r) > P^{\alpha}_{\max}(\mathrm{C};r)$. At small r, it depends on which probability, $P\left\{\mathrm{H}_\alpha\right\}$ or $P\left\{\mathrm{H}_\beta\right\}$ is bigger: if *a)* $P\left\{\mathrm{H}_\beta\right\} > P\left\{\mathrm{H}_\alpha\right\}$ then $P^{\beta}_{\min}(\mathrm{C}_1;r) \ge P^{\alpha}_{\max}(\mathrm{C}_1;r)$, otherwise *b)* $P^{\alpha}_{\min}(\mathrm{C}_1;r) > P^{\beta}_{\max}(\mathrm{C}_1;r)$. The probabilities $P^{\beta}_{\max}(\mathrm{C}_1;r)$ and $P^{\beta}_{\min}(\mathrm{C}_1;r)$ decrease as r goes up while $P^{\alpha}_{\min}(\mathrm{C}_1;r)$ and $P^{\alpha}_{\max}(\mathrm{C}_1;r)$ grow. Hence, hypothesis H_α becomes more and more probable but hypothesis H_β is less probable. Starting with a certain r, we get for the case *a)*

$P_{\min}^{\beta}(\mathrm{C}_1;r)<P_{\max}^{\alpha}(\mathrm{C}_1;r)$ but still $P_{\max}^{\beta}(\mathrm{C}_1;r)>P_{\min}^{\alpha}(\mathrm{C}_1;r)$, at which preference is ambiguous, however with a further increase in r hypothesis H_α begins to prevail: $P_{\min}^{\alpha}(\mathrm{C}_1;r)>P_{\max}^{\beta}(\mathrm{C}_1;r)$. As for the case *b)* H_α prevails at all r. When $\mathrm{C}=\mathrm{C}_2$ for the case *a)* hypothesis H_β prevails at all distances: $P_{\min}^{\beta}(\mathrm{C}_2;r)>P_{\max}^{\alpha}(\mathrm{C}_2;r)$; for the case *b)* we get $P_{\min}^{\alpha}(\mathrm{C}_2;r)\geq P_{\max}^{\beta}(\mathrm{C}_2;r)$ at small r, but beginning from some distance the inequalities $P_{\min}^{\alpha}(\mathrm{C}_2;r)<P_{\max}^{\beta}(\mathrm{C}_2;r)$ and $P_{\max}^{\alpha}(\mathrm{C}_2;r)>P_{\min}^{\beta}(\mathrm{C}_2;r)$ are fulfilled, at which preference is not achievable, however in further growth of r we come to $P_{\min}^{\beta}(\mathrm{C}_2;r)>P_{\max}^{\alpha}(\mathrm{C}_2;r)$.

We define identification probabilities (*IP*s) of one $P_{\mathrm{C}}^{\alpha}(r)\equiv P_{\min}^{\alpha}(\mathrm{C};r)$ and of two sources $P_{\mathrm{C}}^{\beta}(r)\equiv P_{\max}^{\beta}(\mathrm{C};r)$ if $P\{\mathrm{H}_\beta\}P_{\mathrm{C}}^{+}(r)<P\{\mathrm{H}_\alpha\}P\{\mathrm{C}|\mathrm{H}_\alpha\}$, and $P_{\mathrm{C}}^{\alpha}(r)\equiv P_{\max}^{\alpha}(\mathrm{C};r)$, $P_{\mathrm{C}}^{\beta}(r)\equiv P_{\min}^{\beta}(\mathrm{C};r)$ if $P\{\mathrm{H}_\beta\}P_{\mathrm{C}}^{-}(r)>P\{\mathrm{H}_\alpha\}P\{\mathrm{C}|\mathrm{H}_\alpha\}$. *IP*s are not defined if $P_{\mathrm{C}}^{-}(r)\leq P\{\mathrm{C}|\mathrm{H}_\alpha\}P\{\mathrm{H}_\alpha\}/P\{\mathrm{H}_\beta\}\leq P_{\mathrm{C}}^{+}(r)$. To select a hypothesis when one *IP* marginally differs from another threshold function $\delta_H(r;\mathrm{C})$ of relative difference between *IP*s is compiled:

$$\delta_H(r;\mathrm{C})=\begin{cases}\dfrac{P\{\mathrm{H}_\alpha\}P\{\mathrm{C}|\mathrm{H}_\alpha\}}{P\{\mathrm{H}_\beta\}P_{\mathrm{C}}^{-}(r)}-1, P\{\mathrm{H}_\beta\}P_{\mathrm{C}}^{-}(r)>P\{\mathrm{H}_\alpha\}P\{\mathrm{C}|\mathrm{H}_\alpha\}\\ 1-\dfrac{P\{\mathrm{H}_\beta\}P_{\mathrm{C}}^{+}(r)}{P\{\mathrm{H}_\alpha\}P\{\mathrm{C}|\mathrm{H}_\alpha\}}, P\{\mathrm{H}_\beta\}P_{\mathrm{C}}^{+}(r)<P\{\mathrm{H}_\alpha\}P\{\mathrm{C}|\mathrm{H}_\alpha\}\end{cases}.$$

It is compared with a threshold $t_H>0$: at $|\delta_H(r;\mathrm{C})|<t_H$ preference is ambiguous; if $\delta_H(r;\mathrm{C})\geq t_H$ then we select H_α, if $\delta_H(r;\mathrm{C})\leq -t_H$ H_β is preferred.

To summarize the results of Section 4 we present the core pseudocode of the identification procedure:

if $P_{\mathrm{C}}^{-}(r)\leq P\{\mathrm{C}|\mathrm{H}_\alpha\}P\{\mathrm{H}_\alpha\}/P\{\mathrm{H}_\beta\}\leq P_{\mathrm{C}}^{+}(r)$

then *No preference of a hypothesis* **else**

if $\delta_H(r;\mathrm{C})\geq t_H$ **then** *Prefer* H_α

else if $\delta_H(r;\mathrm{C})\leq -t_H$ **then** *Prefer* H_β

else *No preference of a hypothesis*

end if end if end if

5. Estimation of *R99*

The topic of a confidence circle has been addressed in a number of publications regarding circular error probability (*CEP*) integral, occurring in navigation and surveillance systems [25-29]. *CEP* is the radius of a confidence circle which contains a random variable with probability 0.5.

The probability density for zero mean bivariate Gaussian variable $\mathbf{z}=\begin{bmatrix}x & y\end{bmatrix}^T$ with covariance matrix $\mathbf{K}$ is defined as

$$f_{\mathbf{z}}(\mathbf{z},\mathbf{K})=\frac{1}{2\pi\sqrt{\det\mathbf{K}}}\exp\left(-\frac{1}{2}\mathbf{z}^T\mathbf{K}^{-1}\mathbf{z}\right),\ \mathbf{K}=\begin{bmatrix}\sigma_x^2 & \rho_{\mathrm{cv}}\\ \rho_{\mathrm{cv}} & \sigma_y^2\end{bmatrix}, \tag{10}$$

where σ_x, σ_y and ρ_{cv} are standard deviations and covariance of components x and y. Function (10) is rewritten as

$$f_{xy}(x,y)=\frac{1}{2\pi\sigma_x\sigma_y\sqrt{1-\rho^2}}\exp\left[-\frac{1}{2(1-\rho^2)}\left(\frac{x^2}{\sigma_x^2}-\frac{2\rho xy}{\sigma_x\sigma_y}+\frac{y^2}{\sigma_y^2}\right)\right], \tag{11}$$

where $\rho=\rho_{cv}/(\sigma_x\sigma_y)$ is a correlation coefficient.

Among others, Krempasky *CEP* estimator is the most attractive both owing to its numerical simplicity (it is closed-form) and accuracy (the deviation of *CEP* estimate from exact value is less than 2 percent) [29]. He first rotates coordinates x, y in *CEP* integral with integrand (11) by the angle Γ:

$$\mathrm{tg}\Gamma=\left(\sigma_y^2-\sigma_x^2\right)^{-1}\left[-2\rho_{cv}+\sqrt{4\rho_{cv}^2+\left(\sigma_y^2-\sigma_x^2\right)^2}\right],$$

such that $\sigma_x'^2=\sigma_y'^2=\sigma'^2=\sigma_x^2\cos^2\Gamma+\sigma_y^2\sin^2\Gamma+\rho_{cv}\sin2\Gamma$, $\rho'=(\sigma')^{-2}\left[0.5\left(\sigma_y^2-\sigma_x^2\right)\sin2\Gamma+\rho_{cv}\cos2\Gamma\right]$ in transformed coordinates. With polar coordinates it is written with angular coordinate ϑ after the integral is performed over radial coordinate:

$$0.5=\int_o^{2\pi}\mathrm{d}\vartheta\left\{\frac{-1}{2\pi\varpi\sqrt{1-\rho'}}\left[\exp\left(-\frac{\varpi CEP^2}{2(\sigma')^2}\right)-1\right]\right\},\ \varpi=\frac{1-\rho'\sin\vartheta}{1-\rho'^2}. \tag{12}$$

The integral (12) is expanded to the fourth order in the correlation coefficient ρ', and after much manipulation the final *CEP* estimate is found to be

$$CEP=CEP_{00}\left[1-0.5C_2\rho'^2-0.5\left(C_4+0.25C_2^2\right)\rho'^4\right],\ CEP_{00}=\sqrt{2\ln2}\sigma',\ C_2=0.5-0.25\ln2,$$
$$C_4=C_2\left(\ln2-0.25\ln^2 2-0.5\right)-0.5C_2^2\ln2-0.5625\ln2+0.1875\ln^2 2-0.015625\ln^3 2+0.375. \tag{13}$$

We substitute 0.5 with 0.99 in (12) to rework *CEP* estimator to estimate *R99*. Repeating the same manipulation as in [29], one can make sure that *R99* estimate is deduced from (13) by substitution $\ln2$ with $2\ln10$. Final expression for $R99_K$ will be

$$R99_K=R_0\left[1-0.5B_2\rho'^2-0.5\left(B_4+0.25B_2^2\right)\rho'^4\right],\ R_0=2\sqrt{\ln10}\sigma',\ B_2=0.5(1-\ln10),$$
$$B_4=B_2\left(2\ln10-\ln^2 10-0.5\right)-B_2^2\ln10-1.125\ln10+0.75\ln^2 10-0.125\ln^3 10+0.375.$$

To assess the performance of $R99_K$ we propose the alternate estimate $R99_A$ based on the two specific behaviors of the integrand (10) in probability integral $0.99=\int_{\|\mathbf{z}\|\le R99}f_{\mathbf{z}}(\mathbf{z},\mathbf{K})\mathrm{d}\mathbf{z}$ in the vicinity of zero and beyond. Initially, it is reformulated as an integral along one variable [21]:

$$0.99=\int_0^{R99}F(s)\,\mathrm{d}s\,,\; F(s)=\frac{s}{\sqrt{\lambda_1\lambda_2}}\exp\left\{-\left(\frac{1}{4\lambda_1}+\frac{1}{4\lambda_2}\right)s^2\right\}I_0\left\{\left(\frac{1}{4\lambda_2}-\frac{1}{4\lambda_1}\right)s^2\right\},\tag{14}$$

where $\lambda_1>\lambda_2>0$ are eigenvalues of $\mathbf{K}$, $\lambda_1,\lambda_2=0.5\times\left[\sigma_x^2+\sigma_y^2\pm\sqrt{\left(\sigma_x^2-\sigma_y^2\right)^2+4\rho_{\mathrm{cv}}^2}\right]$; $I_0(\bullet)$ is a modified Bessel function of the first kind and zero order. It is approximated with the use of asymptotic expansions [30]:

$$I_0\left(\Omega s^2\right)\approx\begin{cases}1+\dfrac{\Omega^2s^4}{1\times4}+\dfrac{\Omega^4s^8}{1\times2\times32}+\dfrac{\Omega^6s^{12}}{1\times2\times3\times128}+\ldots,s\le R_\lambda\\ \wp(s)\left(1+\dfrac{1^2}{1!8^1\Omega s^2}+\dfrac{1\times3^2}{2!8^2\Omega^2s^4}+\dfrac{1\times3^2\times5^2}{3!8^3\Omega^3s^6}+\ldots\right),s>R_\lambda\end{cases},\;\Omega\equiv\frac{\lambda_1-\lambda_2}{4\lambda_1\lambda_2},\;\wp(s)\equiv\frac{\exp\left(\Omega s^2\right)}{s\sqrt{2\pi\Omega}},\;R_\lambda=2\sqrt{\frac{\lambda_1\lambda_2}{\lambda_1-\lambda_2}}.\tag{15}$$

Equation (14) at $R99\le R_\lambda$ (***i***) is rewritten as $0.99=J_0^{R99}$, $J_0^{R99}=\int_0^{R99}F(s)\,\mathrm{d}s$ or at $R99>R_\lambda$ (***ii***) as $0.99=J_0^{R_\lambda}+J_{R_\lambda}^{R99}$, $J_0^{R_\lambda}=\int_0^{R_\lambda}F(s)\,\mathrm{d}s$, $J_{R_\lambda}^{R99}=\int_{R_\lambda}^{R99}F(s)\,\mathrm{d}s$. Integral $J_0^{R_\lambda}$ for (***i***) is the probability which is bigger than or equal to 0.99, i.e. $\mu=0.99-J_0^{R_\lambda}\le0$, then for (***ii***) – $\mu>0$. We use representation (15) at $s\le R_\lambda$ instead of $I_0\left(\Omega s^2\right)$ in integral $J_0^{R_\lambda}$ to get its approximation $\widehat{J}_0^{R_\lambda}$ and $\widehat{\mu}=0.99-\widehat{J}_0^{R_\lambda}$ afterwards. If $\widehat{\mu}\le0$ then case (***i***) is recognized, otherwise– case (***ii***) for which representation from (15) at $s>R_\lambda$ is used instead of $I_0\left(\Omega s^2\right)$ in integral $J_{R_\lambda}^{R99}$ to achieve approximation $\widehat{J}_{R_\lambda}^{R99_A}$. By doing this, we come to the approximation of the right part of (14):

$$0.99=\begin{cases}\widehat{J}_0^{R99_A} & (i):\widehat{\mu}\le0\\ \widehat{J}_0^{R_\lambda}+\widehat{J}_{R_\lambda}^{R99_A} & (ii):\widehat{\mu}>0\end{cases},$$

where $\widehat{J}_0^{R99_A}$ is the same approximation as $\widehat{J}_0^{R_\lambda}$ with $R99_A$ instead of R_λ. The integration techniques detailed in Appendixes lead to the following analytical expressions:

$$\widehat{J}_0^{B}=\frac{2\sqrt{\lambda_1\lambda_2}}{\lambda_1+\lambda_2}\left\{1+\sum_1^{M_0}\frac{\Omega^{2k}}{k!2^{3k-1}}4k(4k-2)\ldots4\times2\gamma^{2k}-e^{-\frac{\eta}{2\gamma}}\left(\sum_1^{M_0}\frac{\Omega^{2k}}{k!2^{3k-1}}\left\{\eta^{2k}+4k\gamma\eta^{2k-1}+\ldots+4k(4k-2)\ldots4\times2\gamma^{2k}\right\}+1\right)\right\},$$

$$\gamma=2\lambda_1\lambda_2/(\lambda_1+\lambda_2),\;\eta\equiv B^2,\;B\in\left\{R_\lambda,R99_A\right\},$$

see Appendix A, and

$$\widehat{J}_{R_\lambda}^{R99}=\sqrt{\frac{\lambda_1}{\lambda_1-\lambda_2}}\left\{\left[erf\left(\frac{R99_A}{\sqrt{2\lambda_1}}\right)-erf\left(\frac{R_\lambda}{\sqrt{2\lambda_1}}\right)\right]\left[1+\sum_{k=1}^{M_\infty}\frac{(-2)^k\prod_{s=1}^{k}(2s-1)^2}{(16\lambda_1\Omega)^k\,k!\prod_{s=1}^{k}\left[2(k-s)+1\right]}\right]+\right.$$

$$\left.+\frac{2}{\sqrt{\pi}}\sum_{k=1}^{M_\infty}\frac{\prod_{s=1}^{k}(2s-1)^2}{(16\lambda_1\Omega)^k\,k!}\sum_{\ell=1}^{k}\frac{(-2)^{\ell-1}}{\prod_{s=1}^{\ell}\left[2(k-s)+1\right]}\left[\frac{\exp\left(-\frac{R_\lambda^2}{2\lambda_1}\right)}{\left(\frac{R_\lambda}{\sqrt{2\lambda_1}}\right)^{2(k-\ell)+1}}-\frac{\exp\left(-\frac{R99_A^2}{2\lambda_1}\right)}{\left(\frac{R99_A}{\sqrt{2\lambda_1}}\right)^{2(k-\ell)+1}}\right]\right\},$$

where $erf(R)=\frac{2}{\sqrt{\pi}}\int_0^R e^{-s^2}ds$, see Appendix B; M_0, M_∞ are the orders of approximation. As $R99_A > R_\lambda$ the member $\frac{\exp\left(-R99_A^2/(2\lambda_1)\right)}{\left(R99_A/\sqrt{2\lambda_1}\right)^{2(k-\ell)+1}}$ in $\widehat{J}_{R_\lambda}^{R99_A}$ is small as compared to $\frac{\exp\left(-R_\lambda^2/(2\lambda_1)\right)}{\left(R_\lambda/\sqrt{2\lambda_1}\right)^{2(k-\ell)+1}}$ and further will be ignored.

We assign $M_0=2$ in $\widehat{J}_0^B$ after that case *(i)* is reduced to the following equation for $R99_A$:

$$e^{-\frac{\eta}{2\gamma}}\left(\sum_1^2\frac{\Omega^{2k}}{k!2^{3k-1}}\left\{\eta^{2k}+4k\gamma\eta^{2k-1}+\ldots+4k(4k-2)\ldots4\times2\gamma^{2k}\right\}+1\right)=1+\sum_1^2\frac{\Omega^{2k}}{k!2^{3k-1}}4k(4k-2)\ldots4\times2\gamma^{2k}-0.99\frac{\lambda_1+\lambda_2}{2\sqrt{\lambda_1\lambda_2}},$$

where $R99_A=\eta^{1/2}$. As it can be observed, the derivative along η of the function from the left side of this equation is negative, supplying the solution uniqueness.

For the case *(ii)* we set $M_\infty=2$ in $\widehat{J}_{R_\lambda}^{R99_A}$ and obtain the closed-form solution:

$$erf\left(\frac{R99_A}{\sqrt{2\lambda_1}}\right)=erf\left(\frac{R_\lambda}{\sqrt{2\lambda_1}}\right)+\frac{\tilde{\mu}\sqrt{\frac{\lambda_1-\lambda_2}{\lambda_1}}-\frac{2\,e^{-\frac{R_\lambda^2}{2\lambda_1}}}{\sqrt{\pi}}\sum_{k=1}^{2}\frac{\prod_{s=1}^{k}(2s-1)^2}{(16\lambda_1\Omega)^k\,k!}\sum_{\ell=1}^{k}\frac{(-2)^{\ell-1}}{\left(\frac{R_\lambda}{\sqrt{2\lambda_1}}\right)^{2(k-\ell)+1}\prod_{s=1}^{\ell}\left[2(k-s)+1\right]}}{1+\sum_{k=1}^{2}\frac{(-2)^k\prod_{s=1}^{k}(2s-1)^2}{(16\lambda_1\Omega)^k\,k!\prod_{s=1}^{k}\left[2(k-s)+1\right]}}.$$

The performance of estimate $R99_K$ versus $R99_A$ is studied by simulation in the full range of $\widehat{\mu}$ from -0.0098 to 0.9888, which corresponds to varying of the correlation coefficient and sigma ratio (ratio of smaller to larger standard deviation) in the intervals (-1,1) and (0,1) respectively. The performance index is the probability integral (14) performed numerically with estimates $R99_K$ and $R99_A$. Table 1 contains the extraction from the simulation results.

$\widehat{\mu}$	$\int_0^R F(s)\,\mathrm{d}s, R \in \{R99_K, R99_A\}$ Krempasky	Alternate	$\left(\frac{R99_K}{R99_A} - 1\right) \times 100$
-0.0098	0.9900	0.9900	0.00
-0.0097	0.9899	0.9899	0.00
-0.0064	0.9899	0.9897	0.12
-0.0032	0.9899	0.9880	1.90
0.0014	0.9900	0.9921	-2.50
0.0086	0.9898	0,9874	2.70
0.1083	0.9900	0.9875	2.70
0.1446	0.9899	0.9880	2.40
0.1985	0.9902	0.9887	1.90
0.2502	0.9903	0.9893	1.30
0.3045	0.9906	0.9899	0.85
0.4009	0.9911	0.9909	0.19
0.4346	0.9912	0.9912	0.00
0.5112	0.9916	0.9916	0.00
0.5429	0.9916	0.9916	0.00
0.5862	0.9917	0.9915	0.22
0.6115	0.9917	0.9915	0.33
0.6465	0.9919	0.9914	0.60
0.7025	0.9921	0.9914	1.00
0.7949	0.9925	0.9911	1.80
0.8512	0.9926	0.9909	2.70
0.8840	0.9926	0.9905	3.10
0.9208	0.9927	0.9905	3.50
0.9794	0.9932	0.9900	4.40
0.9867	0.9958	0.9900	5.40
0.9883	0.9967	0.9900	6.50

Table 1: Simulation Results on Performance of $R99_K$ versus $R99_A$.

As we can see from the Table 1, at $\widehat{\mu} < 0$ estimates $R99_K$ and $R99_A$ are both of excellent accuracy and close to each other. As $\widehat{\mu}$ approaches zero from below, $R99_K$ keeps excellent accuracy while $R99_A$ degrades. The bigger $\widehat{\mu}$ after zero is, the better $R99_A$ becomes, while $R99_K$ degrades gradually. It is safe to conclude, that $R99_A$ begins to outperform $R99_K$ visibly from the $\widehat{\mu} \approx 0.8$ onwards. As a result, radius *R99* is estimated as follows:

$$R99 = \begin{cases} R99_K, \widehat{\mu} \le 0.8 \\ R99_A, \widehat{\mu} > 0.8 \end{cases}.$$

6. The Distinguishing Two Location Estimates between One or Two close users of the TDOA BSs Network

The technique is applied to distinguish two planar positional estimates of the user(s) of TDOA BSs network. The received signals are classified by parameter q with the probabilities $\{P_j^I\}_{j=1}^{j=Q}$ and $\{P_j^{II}\}_{j=1}^{j=Q}$ over the emissions *I* and *II*, where Q is the number of different users. Proceeding from these probabilities, one can easily derive $P\{\mathrm{H}_\alpha\}=\sum_{j=1}^{Q} P_j^I P_j^{II}$ and $P\{\mathrm{H}_\beta\}=1-P\{\mathrm{H}_\alpha\}$.

In TDOA scheme, output signal at k-th BS is with parameter τ_k of time difference of emission arrival on that BS and reference one, placed in (0, 0), from a user located at $\boldsymbol{\varphi}$: $p_k(\boldsymbol{\varphi})=c\tau_k(\boldsymbol{\varphi})=\|\boldsymbol{\varphi}-\boldsymbol{\varphi}_k\|-\|\boldsymbol{\varphi}\|$, $k=\overline{1,L_p}$, $L_p=L-1$, where c is the speed of light. The model (1) is here reduced to the following one:

$$\begin{gathered}\nu\left(t^I;\boldsymbol{q}^I,p_k\left(\boldsymbol{\varphi}^I\right)\right)=g\left(t^I-c^{-1}p_k\left(\boldsymbol{\varphi}^I\right);\boldsymbol{q}^I\right)+n_k\left(t^I\right),\\ \nu\left(t^{II};\boldsymbol{q}^{II},p_k\left(\boldsymbol{\varphi}^{II}\right)\right)=g\left(t^{II}-c^{-1}p_k\left(\boldsymbol{\varphi}^{II}\right);\boldsymbol{q}^{II}\right)+n_k\left(t^{II}\right),\\ \nu\left(t^I;\boldsymbol{q}^I\right)=g\left(t^I;\boldsymbol{q}^I\right)+n_L\left(t^I\right),\nu\left(t^{II};\boldsymbol{q}^{II}\right)=g\left(t^{II};\boldsymbol{q}^{II}\right)+n_L\left(t^{II}\right)\end{gathered}$$

with scalar signals, waveforms and noises instead of vector ones as in (1). Scalar processes $\nu(t;\boldsymbol{q})$, $n_L(t)$ and function $g(t;\boldsymbol{q})$ with $p_L=0$ are given at reference BS.

Maximum likelihood estimator $\Im_p$ is efficient asymptotically if a signal at each of L_p BSs is uncorrelated with the signal at reference BS: $E\{n_k(t)n_L(t)\}=0$ [31]. As far as $\Im_\varphi$ is concerned, the constrained weighted least square estimator, which combine core pillars of quadratic and linear correction techniques, is efficient for uncorrelated measurement errors $\Delta\tau_k$ of parameters τ_k, $\boldsymbol{\upsilon}=\left[\Delta\tau_1,\ldots,\Delta\tau_{L_p}\right]^T$ [32-34]. Despite the fact that they nevertheless correlate through signal at reference BS, we presume that matrix $E\{\boldsymbol{\upsilon}\boldsymbol{\upsilon}^T\}$ is to be near to a diagonal one. Reasoning from the aforementioned, the covariance matrix in TDOA BSs network is calculated as

$$\boldsymbol{\Phi}(\boldsymbol{\varphi})=\left(\left[\frac{\partial c\boldsymbol{\tau}(\boldsymbol{\varphi})}{\partial\boldsymbol{\varphi}}\right]^T diag\left\{\frac{1}{\sigma_k^2}\right\}_1^{L_p}\left[\frac{\partial c\boldsymbol{\tau}(\boldsymbol{\varphi})}{\partial\boldsymbol{\varphi}}\right]\right)^{-1},\ \boldsymbol{\tau}(\boldsymbol{\varphi})=\left[\tau_1(\boldsymbol{\varphi}),\ldots,\tau_{L_p}(\boldsymbol{\varphi})\right]^T,\ \sigma_k^2=E\left\{\left(c\Delta\tau_k\right)^2\right\}.$$

There are five BSs, including the reference BS. Four BSs in conjunction with the reference one, produce the range differences of arrival $c\tau_k$, corrupted by the noises with standard deviation $\sigma_1=\sigma_2=\sigma_3=\sigma_4=$ 0.04m (m hereinafter refers to meters). They are situated at (1000, -700)m, (-1000, 2000)m, (4000, 3000)m and (-4000, 1000)m. The technique is being tested in the close users domain (CUD), which encompasses the position $\boldsymbol{\varphi}_1$ placed at (14000, 12600)m, with the using of approximations of function $SRL(\boldsymbol{\varphi}_2)$ and matrix-function $\mathbf{W}_\psi(\boldsymbol{\varphi}_2)$ in CUD by the constant values.

Since the exact solution for the distribution of $\|\boldsymbol{\psi}\|^2$ is very expensive, the simpler closed-form approximation is utilized in the study [24,35].

6.1. Characterization of the CUD

The CUD is thought to be described by the constant characteristics *SRL* and **W** which would be sufficient approximations of $SRL(\varphi_2) = R99_1 + R99(\varphi_2)$, where $R99_1$ and $R99(\varphi_2)$ are the radii of the confidence circles S_1 and S_2 of probability 0.99, and of $\mathbf{W}_\psi(\varphi_2) = \mathbf{\Phi}(\varphi_1) + \mathbf{\Phi}(\varphi_2)$ for the all φ_2 from CUD. Below we establish the domain where both $SRL(\varphi_2)$ and $\mathbf{W}_\psi(\varphi_2)$ are varying negligibly and find out their approximations *SRL* and **W**.

In the simulation, $R99(\varphi_2)$ is computed at N points $\{\varphi_2^k\}$ evenly spaced along the circumference with radius r centered at φ_1 : $R99_2^k(r) = R99(\varphi_2^k)\big|_{\|\varphi_2^k - \varphi_1\| = r}$, $k = \overline{1, N}$. Thereafter, mean values $\overline{R99}_2(r) = N^{-1}\sum_{k=1}^{N} R99_2^k(r)$, $\overline{SRL}(r) = R99_1 + \overline{R99}_2(r)$ and the square root from the mean of squared deviations of $R99_2^k(r)$ from $\overline{R99}_2(r)$, $\bar{\varepsilon}(r) = \sqrt{N^{-1}\sum_{k=1}^{N}\left(R99_2^k(r) - \overline{R99}_2(r)\right)^2}$ are determined. We start with $r^{(1)} = R99_1$, and obtain $\overline{SRL}(r^{(1)})$, $\bar{\varepsilon}(r^{(1)})$. $SRL(\varphi_2)$ at $r \le r^{(1)}$ is approximated by $\overline{SRL}(r^{(1)})$ with accuracy $\bar{\varepsilon}(r^{(1)})$. Next distance $r^{(2)} = \overline{SRL}(r^{(1)})$ is to find $\overline{SRL}(r^{(2)})$ with $\bar{\varepsilon}(r^{(2)})$. If $\overline{SRL}(r^{(2)}) \approx \overline{SRL}(r^{(1)})$ then $SRL(\varphi_2)$ in the region of $r \le r^{(2)}$ is approximated by $\overline{SRL}(r^{(2)})$ with accuracy $\bar{\varepsilon}(r^{(2)})$. This region is the CUD subdomain where separation can be smaller than or close to $\overline{SRL}(r^{(2)})$. If $\overline{SRL}(r^{(4)}) \approx \overline{SRL}(r^{(3)}) \approx \overline{SRL}(r^{(2)})$ at some $r^{(3)} > r^{(2)}$ and at $r^{(4)} > r^{(3)}$ then $SRL(\varphi_2)$ is approximated by $\overline{SRL}(r^{(3)})$ in the subdomain $r \le r^{(3)}$, and at $r \le r^{(4)}$ we acquire entire CUD with $SRL = \overline{SRL}(r^{(4)}) \pm \bar{\varepsilon}(r^{(4)})$. The simulation results for $R99_1$=14.5133m at N =1000 are given in the Table 2.

Subdomain	Distance r	$\overline{R99}_2(r)$	$\overline{SRL}(r)$	$\bar{\varepsilon}(r)$
↑	14.5133m	14.5133m	29.0266m	0.0253m
$r \le SRL$	29.0266m	14.5132m	29.0265m	0.0507m
$r > SRL$	33m	14.5132m	29.0265m	0.0576m
↓	38m	14.5132m	29.0265	0.0664m

Table 2: CUD Characterization on *SRL*.

Taking into consideration the column $\bar{\varepsilon}(r)$ from the Table 2, we infer that $SRL(\varphi_2) \in$[28.9601, 29.0929]m. Having interval where true $SRL(\varphi_2)$ is varied, we accept it to be constant, namely *SRL*=29.02m with the accuracy $\pm$0.07m. Thus, $SRL(\varphi_2)$ is approximated in CUD by the constant with a good accuracy. Therefore, we have reason to approximate the true covariance matrices $\mathbf{W}_\psi(\varphi_2)$ by a constant matrix everywhere in CUD as well. To this end, the mean of $\mathbf{\Phi}(\varphi_2)$ over 1000 points evenly spaced along the circumference of radius $r^{(4)}$, $\overline{\mathbf{\Phi}}_2 = 10^{-3}\sum_{k=1}^{1000}\mathbf{\Phi}(\varphi_2^k)\big|_{\|\varphi_2^k - \varphi_1\| = r^{(4)}}$, and $\overline{\mathbf{W}} = \mathbf{\Phi}(\varphi_1) + \overline{\mathbf{\Phi}}_2$ are computed. To reveal the scattering of $\mathbf{W}_\psi(\varphi_2)$ towards $\overline{\mathbf{W}}$ we additionally determine the matrices $\mathbf{W}_{\min} = \mathbf{\Phi}(\varphi_1) + \mathbf{\Phi}(\varphi_{2\min})$, $\mathbf{W}_{\max} =$ $= \mathbf{\Phi}(\varphi_1) + \mathbf{\Phi}(\varphi_{2\max})$, where $\varphi_{2\min}$, $\varphi_{2\max}$ correspond to the minimum and maximum of $R99(\varphi_2)$ on the same circumference: $\varphi_{2\min} = \arg\min\left\{R99_2^k\left(r^{(4)}\right)\right\}_1^{1000}$, $\varphi_{2\max} = \arg\max\left\{R99_2^k\left(r^{(4)}\right)\right\}_1^{1000}$. Simulation data in square meters at $\mathbf{\Phi}(\varphi_1) = \begin{bmatrix} 19.2589 & 15.2837 \\ 15.2837 & 12.1876 \end{bmatrix}$ are:

$$\overline{\mathbf{\Phi}}_2 = \begin{bmatrix} 19.2593 & 15.2837 \\ 15.2837 & 12.1874 \end{bmatrix},\ \overline{\mathbf{W}} = \begin{bmatrix} 38.5182 & 30.5673 \\ 30.5673 & 24.3749 \end{bmatrix};\ \mathbf{W}_{\min} = \begin{bmatrix} 38.2219 & 30.3798 \\ 30.3798 & 24.2637 \end{bmatrix},\ \mathbf{W}_{\max} = \begin{bmatrix} 38.8155 & 30.7555 \\ 30.7555 & 24.4864 \end{bmatrix}.$$

Following the logic in characterization on *SRL*, we approximate $\mathbf{W}_{\psi}(\boldsymbol{\varphi}_2)$ by the matrix $\mathbf{W}=\begin{bmatrix} 38.51 & 30.56 \\ 30.56 & 24.37 \end{bmatrix}$ with the accuracy $\pm\begin{bmatrix} 0.30 & 0.19 \\ 0.19 & 0.11 \end{bmatrix}$. Spectral characteristic $\bar{e}$ of **W** is equal to 29.3636, hence $0.4842 < PRI_S < 0.4905$.

6.2. Identifying in the CUD

We set distance r varying it throughout the CUD and simulate desired *IP*s for each event $\mathrm{C}\in\{\mathrm{C}_1,\mathrm{C}_2\}$ with *SRL* and **W** obtained in Subsection 6.1. The simulation is conducted for prior probabilities $P\{\mathrm{H}_\alpha\}$=0.2, 0.48, 0.5, 0.52, 0.8 and related $P\{\mathrm{H}_\beta\}$=0.8, 0.52, 0.5, 0.48, 0.2. The results are shown in Table 3, where α, β and δ denote the rows for *IP*s $P_{\mathrm{C}}^{\alpha}(r)$, $P_{\mathrm{C}}^{\beta}(r)$ and the function $\delta_H(r;\mathrm{C})$ respectively; abbreviation "*undef*" denotes undefined *IP*s and $\delta_H(r;\mathrm{C})$. The numerical values are rounded to the third and if necessary to the fourth decimal place. To test a hypothesis threshold t_H=0.05 is chosen. The fragments of rows δ that are colored blue conform to the one user identification, those colored brown conform to the two user identification, and the uncolored ones do not conform to any identification. Green column is to highlight the neighborhood of *SRL*.

Remark 2. The distance r is varying in Table 3 from 2m till 34.6m. It does not contain the results of computation with $P\{\mathrm{H}_\alpha\}$=0.52 at negligible distance for $\mathrm{C}=\mathrm{C}_2$: one user is identified at $r\le 0.5$ with $P_{\mathrm{C}_2}^{\alpha}(0.5)$=0.510, $P_{\mathrm{C}_2}^{\beta}(0.5)$=0.490 and $\delta_H(0.5;\mathrm{C}_2)$=0.051; in the range from 0.5 till 0.8 identification is rejected with $P_{\mathrm{C}_2}^{\alpha}(0.8)$=0.503, $P_{\mathrm{C}_2}^{\beta}(0.8)$=0.497 and $\delta_H(0.8;\mathrm{C}_2)$ =0.012; from 0.9 till 2 and further up to 2.6m identification probabilities are not defined.

			Distance between users *r* [m]																	
			r* < *SRL															***r* > *SRL***		
P{Hα}			2	2.6	3.5	4.1	5.4	7	10	13	15	20	25	26	26.5	27.5	28.5	29.5	32	34.6
0.2	C_1	α	0.200	0.200	0.200	0.200	0.200	0.200	0.201	0.203	0.206	0.223	0.268	0.283	0.291	0.308	0.329	*undef*	*undef*	0.514
		β	0.800	0.800	0.800	0.800	0.800	0.800	0.799	0.797	0.794	0.777	0.732	0.717	0.709	0.692	0.671	*undef*	*undef*	0.486
		δ	-0.750	-0.750	-0.750	-0.750	-0.750	-0.750	-0.749	-0.746	-0.741	-0.713	-0.633	-0.606	-0.590	-0.554	-0.510	*undef*	*undef*	0.054
	C_2	α	0.195	0.191	0.184	0.179	0.164	0.143	0.099	0.058	0.037	0.008	0.001	0.001	0.0005	0.0003	0.0002	0.0001	0.0001	0.0001
		β	0.805	0.809	0.816	0.821	0.836	0.857	0.901	0.942	0.963	0.992	0.999	0.999	0.9995	0.9997	0.9998	0.9999	0.9999	0.9999
		δ	-0.758	-0.763	-0.774	-0.782	-0.803	-0.833	-0.890	-0.938	-0.962	-0.992	-0.999	-0.999	-0.999	-0.999	-0.999	-0.999	-0.999	-0.999
0.48	C_1	α	0.480	0.480	0.480	0.480	0.480	0.480	0.481	0.484	0.489	*undef*	*undef*	0.505	0.514	0.543	0.607	0.667	0.729	0.796
		β	0.520	0.520	0.520	0.520	0.520	0.520	0.519	0.516	0.511	*undef*	*undef*	0.495	0.486	0.457	0.393	0.333	0.271	0.204
		δ	-0.077	-0.077	-0.077	-0.077	-0.076	-0.075	-0.072	-0.061	-0.045	*undef*	*undef*	0.021	0.053	0.160	0.354	0.501	0.629	0.744
	C_2	α	0.472	0.466	0.455	0.446	0.421	0.382	0.288	0.185	0.124	0.030	0.004	0.002	0.002	0.001	0.001	0.0004	0.0004	0.0003
		β	0.528	0.534	0.545	0.554	0.579	0.618	0.712	0.815	0.876	0.970	0.996	0.998	0.998	0.999	0.999	0.9996	0.9996	0.9997
		δ	-0.107	-0.127	-0.165	-0.196	-0.273	-0.383	-0.595	-0.773	-0.858	-0.969	-0.996	-0.998	-0.998	-0.999	-0.999	-0.999	-0.999	-0.999

0.5	C_1	α	0.500	0.500	0.500	0.500	0.500	0.500	0.500	0.500	0.500	0.502	0.515	0.525	0.534	0.563	0.626	0.685	0.745	0.809
		β	0.500	0.500	0.500	0.500	0.500	0.500	0.500	0.500	0.500	0.498	0.485	0.475	0.466	0.437	0.374	0.315	0.255	0.191
		δ	0.000	0.000	0.000	0.000	0.0000	0.0001	0.0003	0.0007	0.001	0.007	0.058	0.096	0.126	0.225	0.403	0.539	0.657	0.764
	C_2	α	0.492	0.486	0.475	0.466	0.440	0.401	0.305	0.198	0.133	0.033	0.004	0.003	0.002	0.001	0.001	0.0005	0.0004	0.0003
		β	0.508	0.514	0.525	0.534	0.560	0.599	0.695	0.802	0.867	0.967	0.996	0.997	0.998	0.999	0.999	0.9995	0.9996	0.9997
		δ	-0.032	-0.054	-0.095	-0.129	-0.213	-0.331	-0.562	-0.754	-0.846	-0.966	-0.996	-0.997	-0.998	-0.999	-0.999	-0.999	-0.999	-0.999
0.52	C_1	α	0.520	0.520	0.520	0.520	0.520	0.520	0.520	0.520	0.520	0.522	0.535	0.545	0.553	0.583	0.645	0.702	0.760	0.821
		β	0.480	0.480	0.480	0.480	0.480	0.480	0.480	0.480	0.480	0.478	0.465	0.455	0.447	0.417	0.355	0.298	0.240	0.179
		δ	0.077	0.077	0.077	0.077	0.077	0.077	0.077	0.078	0.078	0.084	0.131	0.166	0.193	0.284	0.449	0.575	0.684	0.782
	C_2	α	*undef*	*undef*	0.495	0.486	0.460	0.420	0.322	0.211	0.143	0.035	0.005	0.003	0.002	0.001	0.0007	0.0005	0.0004	0.0004
		β	*undef*	*undef*	0.505	0.514	0.540	0.580	0.678	0.789	0.857	0.965	0.995	0.997	0.998	0.999	0.9993	0.9995	0.9996	0.9996
		δ	*undef*	*undef*	-0.020	-0.056	-0.147	-0.276	-0.525	-0.733	-0.834	-0.963	-0.995	-0.997	-0.998	-0.999	-0.999	-0.999	-0.999	-0.999
0.8	C_1	α	0.800	0.800	0.800	0.800	0.800	0.800	0.800	0.800	0.800	0.801	0.809	0.816	0.821	0.838	0.870	0.897	0.921	0.944
		β	0.200	0.200	0.200	0.200	0.200	0.200	0.200	0.200	0.200	0.199	0.191	0.184	0.179	0.162	0.130	0.103	0.079	0.056
		δ	0.750	0.750	0.750	0.750	0.750	0.750	0.750	0.750	0.750	0.752	0.765	0.774	0.782	0.806	0.851	0.885	0.914	0.941
	C_2	α	0.741	0.709	0.654	0.611	0.504	*undef*	*undef*	0.496	0.381	0.119	0.017	0.010	0.008	0.004	0.002	0.0019	0.0015	0.0013
		β	0.259	0.291	0.346	0.389	0.496	*undef*	*undef*	0.504	0.619	0.881	0.983	0.990	0.992	0.996	0.998	0.9981	0.9985	0.9987
		δ	0.651	0.590	0.471	0.364	0.015	*undef*	*undef*	-0.014	-0.386	-0.865	-0.983	-0.990	-0.992	-0.996	-0.998	-0.998	-0.998	-0.999

Table 3. Identification Results in the CUD.

Figure 3 visualizes identification probabilities $P^{\alpha}_{C_1}(r)$ and $P^{\beta}_{C_2}(r)$ from Table 3 and in the light of Remark 2.

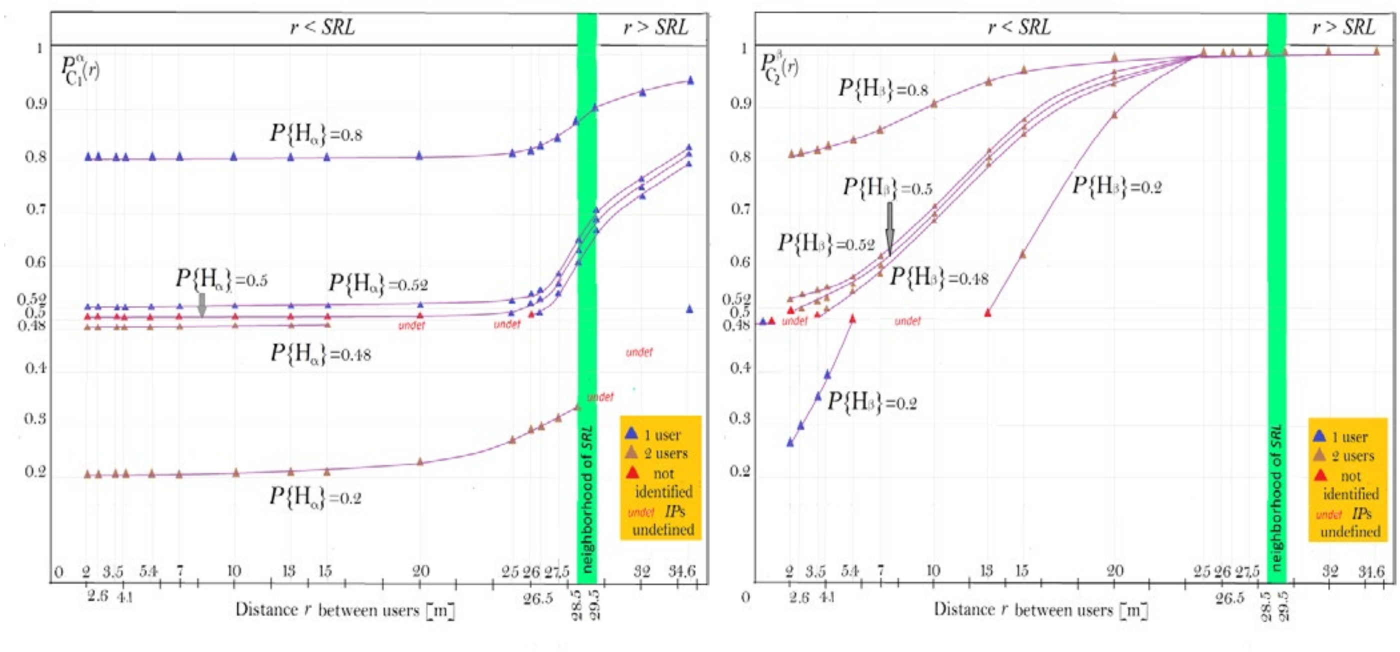

(**a**) (**b**)

Figure 3: Identification probabilities (a) $P^{\alpha}_{C_1}(r)$ and (b) $P^{\beta}_{C_2}(r)$.

6.3. Discussion of the Simulation Results

The behavior of *IP*s as function of separation r depends on the prior probability as parameter and cardinally on what event from Bayes event space happens.

When the prior probability of two-user hypothesis is large enough then at $C = C_1$ identification procedure only recalculates the initial probability in the direction of decrease up to a distance around *SRL* leaving PS-decision unchanged, PS-decision is changed by procedure in favor of one user with some distance over *SRL*; identification does not work between that distances. At $C = C_2$ PS-decision remains unchanged everywhere in CUD with recalculation of initial probability in the direction of increase. If, on the other hand, prior probability of one-user hypothesis is large enough then at $C = C_1$ PS-decision is unchanged in the CUD with a growth of initial probability. At $C = C_2$ PS-decision is unchanged with a descent of initial probability up to some distance below *SRL*, but with some greater distance also below *SRL* PS-decision is changed in favor of two users in the rest of the CUD; between that distances identification does not work.

If the two-user hypothesis is slightly more probable than the one-user one then at $C = C_1$ PS-decision is unchanged with a descent of initial probability up to some distance below *SRL*, but with some greater distance also below *SRL* and further PS-decision is changed in favor of one user; between that distances we may not select a hypothesis. At $C = C_2$ PS-decision is unchanged in the CUD with a growth of initial probability. If the one-user hypothesis is slightly more probable than the two-user one then at $C = C_1$ PS-decision is unchanged in the CUD with a growth of initial probability. At $C = C_2$ initial probability decreases remaining PS-decision to be unchanged only at negligibly small distances, but starting from some short distance it is changed in favor of two users; we may not select a hypothesis between that distances.

For equally probable hypotheses initial probabilities both are equal to 0.5. The probability of one user at $C = C_1$ increases with distance while of two users – decreases. Beginning from big enough distance below *SRL* PS-decision (which is no preference herein) is changed in favor of one user; at smaller distances preference is impossible. The probability of two users at $C = C_2$ increases with distance while of one user – decreases. Beginning from small enough distance PS-decision is changed in favor of two users; before that distance preference is impossible.

We can observe that $P_{C_2}^{\beta}(r)$ changes faster than $P_{C_1}^{\alpha}(r)$ in the region of not too much separation. Let us $P_{C_1}(r)$ is either $P_{C_1}^{+}(r)$ or $P_{C_1}^{-}(r)$. Taking into account that $P_{C_2}^{+}(r) = 1 - P_{C_1}^{-}(r)$, $P_{C_2}^{-}(r) = 1 - P_{C_1}^{+}(r)$ it is easy to show that

$$\frac{dP_{C_1}^{\alpha}(r)}{dr} = -P\{H_\alpha\}P\{H_\beta\}\frac{dP_{C_1}(r)}{dr}\Pi_1(r),\ \frac{dP_{C_2}^{\beta}(r)}{dr} = -P\{H_\alpha\}P\{H_\beta\}\frac{dP_{C_1}(r)}{dr}\Pi_2(r),$$

$$\Pi_1(r) = \frac{P\{C_1|H_\alpha\}}{\chi^2(r)},\ \Pi_2(r) = \frac{1 - P\{C_1|H_\alpha\}}{\left[1-\chi(r)\right]^2}\ \chi(r) = P\{H_\alpha\}P\{C_1|H_\alpha\} + P\{H_\beta\}P_{C_1}(r),$$

where $P\{C_1|H_\alpha\}$=0.999749 in our *CUD*. With a decrease in r factors $\Pi_1(r)$ and $\Pi_2(r)$ approach correspondently to $1/P\{C_1|H_\alpha\}$=1/0.999749=1.00025 and to $1/\left(1-P\{C_1|H_\alpha\}\right)$=1/0.000251=3984, so $\Pi_2(r)$ is to be much more than $\Pi_1(r)$ at short r. In particular, this manifests itself in $P_{C_2}^{\beta}(r)$ changes initial preference $P\{H_\alpha\} = P\{H_\beta\}$=0.5 at much smaller separation as compared to how $P_{C_1}^{\alpha}(r)$ does it. With an increase in r factor $\Pi_1(r)$ rises, while factor $\Pi_2(r)$ decreases. We can see from Fig. 3 how the derivative of $P_{C_1}^{\alpha}(r)$ increases visibly around the neighborhood of *SRL* yet the derivative of $P_{C_2}^{\beta}(r)$ decreases as $P_{C_2}^{\beta}(r)$ approaches to its asymptote equal to 1.

7. Concluding Remarks

The novel Bayesian technique aimed to identify one or two closely spaced sources under double emission through the use of location estimates with the approximately equal covariance matrices, which is parameterized by the sources separation, is designed. Prior probabilities of the one/two-sources hypotheses are determined via physical characteristics of the emissions and extracted from the prior solution (abbreviated as PS in the paper), assuming that they can be equally probable.

Functioning of the technique below and over the resolution limit of the estimator is provided by the new resolution criterion emphasizing the probability of the resolving of the planar parameter decoupled estimates (abbreviated as *PRI* in the paper). The resolution limit in this criterion is so called Statistical Resolution Limit (abbreviated as *SRL* in the paper), which is consistent in *PRI* with conventional scalar resolution criteria. It is equal to the sum of the radii of the confidence circles around each parameter in charge of probability 0.99.

Bayes event space consists of two mutually exclusive events: when confidence circles around sample estimates intersect or do not intersect, accordingly when the distance between them is below or over *SRL*. The extreme probabilities of the events conditioned by one/two-sources hypotheses depend on the distance between locations of hypothesized sources which may be taken both below and over *SRL*.

Identification procedure is studied as applied for the distinguishing positional estimates between one and two close users of time difference of arrival basic stations network. The results of the simulation illustrate the mechanism of how it revises PS-decision with distance between users subject to Byes event.

In the future we plan to extend proposed technique on a more general problem of identifying the number of sources, each of which can emit one or several times by a given set of location estimates.

References

1. Xiao, Z., & Yan, Z. (2020, June). Radar emitter identification based on naive Bayesian algorithm. In *2020 IEEE 5th Information Technology and Mechatronics Engineering Conference (ITOEC)* (pp. 1242-1244). IEEE.
2. Tempola, F., Muhammad, M., & Khairan, A. (2018, September). Naive bayes classifier for prediction of volcanic status in indonesia. In *2018 5th International conference on information technology, computer, and electrical engineering (ICITACEE)* (pp. 365-369). IEEE.
3. Bretthorst, G. L., & Smith, C. R. (1989, June). Bayesian analysis of signals from closely-spaced objects. In *Infrared Systems and Components III* (Vol. 1050, pp. 93-104). SPIE.
4. Schodt, D. J., & Lidke, K. A. (2021). Spatiotemporal clustering of repeated super-resolution localizations via linear assignment problem. *Frontiers in Bioinformatics, 1*, 724325.
5. Fazel, M., Wester, M. J., Schodt, D. J., Cruz, S. R., Strauss, S., Schueder, F., ... & Lidke, K. A. (2022). High-precision estimation of emitter positions using Bayesian grouping of localizations. *Nature Communications, 13*(1), 7152.
6. Fazel, M., & Wester, M. J. (2022). Analysis of super-resolution single molecule localization microscopy data: A tutorial. *AIP advances, 12*(1).
7. Smith, S. T. (2005). Statistical resolution limits and the complexified crame/spl acute/r-rao bound. *IEEE Transactions on Signal Processing, 53*(5), 1597-1609.
8. Abramovich, Y. I., Johnson, B. A., & Spencer, N. K. (2009, August). Statistical nonidentifiability of close emitters: Maximum-likelihood estimation breakdown. In *2009 17th European Signal Processing Conference* (pp. 1968-1972). IEEE.
9. Amar, A., & Weiss, A. J. (2008). Fundamental resolution limits of closely spaced random signals. *IET Radar, Sonar & Navigation, 2*(3), 170-179.
10. Abramovich, Y. I., & Johnson, B. A. (2010). Detection–Estimation of Very Close Emitters: Performance Breakdown, Ambiguity, and General Statistical Analysis of Maximum-Likelihood Estimation. *IEEE Transactions on Signal Processing, 58*(7), 3647-3660.
11. Sun, M., Jiang, D., Song, H., & Liu, Y. (2017). Statistical resolution limit analysis of two closely spaced signal sources using Rao test. *IEEE Access, 5,* 22013-22022.
12. Zhang, Y., Zhu, W., Tang, B., Tang, J., Zheng, G., & Bhattacharjya, A. (2018). Angular statistical resolution limit of two closely-spaced point targets: a GLRT-based study. *IEEE Access, 6,* 75924-75936.
13. Liu, P., & Zhang, H. (2021). A mathematical theory of computational resolution limit in multi-dimensional spaces. *Inverse Problems, 37*(10), 104001.
14. Lee, H. B. (1992). The Cramér-Rao bound on frequency estimates of signals closely spaced in frequency. *IEEE Transactions on Signal Processing, 40*(6), 1507-1517.
15. Delmas, J. P., & Abeida, H. (2006, May). Statistical resolution limits of DOA for discrete sources. In *2006 IEEE International Conference on Acoustics Speech and Signal Processing Proceedings* (Vol. 4, pp. IV-IV). IEEE.
16. El Korso, M. N., Boyer, R., Renaux, A., & Marcos, S. (2010, March). Statistical resolution limit for multiple parameters of interest and for multiple signals. In *2010 IEEE International Conference on Acoustics, Speech and Signal Processing* (pp. 3602-3605). IEEE.

17. Wang, Y., Wu, Y., & Shen, Y. (2019). On the resolution limits for MIMO localization. *IEEE Communications Letters, 23*(3), 462-465.
18. Zhang, H., Xu, D., & Wang, N. (2023). Explicit Joint Resolution Limit for Range and Direction-of-Arrival Estimation in MIMO Radar. *IEEE Transactions on Aerospace and Electronic Systems, 59*(5), 5422-5432.
19. Cramér, H. (1999). *Mathematical methods of statistics* (Vol. 26). Princeton university press.
20. Clark, M. P. (1995). On the resolvability of normally distributed vector parameter estimates. *IEEE Transactions on Signal Processing, 43*(12), 2975-2981.
21. Torrieri, D. J. (1984). Statistical theory of passive location systems. *IEEE transactions on Aerospace and Electronic Systems,* (2), 183-198.
22. Delmas, J. P. (2002). Asymptotic performance of second-order algorithms. *IEEE Transactions on Signal Processing, 50*(1), 49-57.
23. Dwight, H. B. (1947). Tables of integrals and other mathematical data. *New York: The MacMillan Company*.
24. Duchesne, P., & De Micheaux, P. L. (2010). Computing the distribution of quadratic forms: Further comparisons between the Liu–Tang–Zhang approximation and exact methods. *Computational Statistics & Data Analysis, 54*(4), 858-862.
25. Gillis, J. T. (1991). Computation of the circular error probability integral. *IEEE Transactions on Aerospace and Electronic Systems, 27*(6), 906-910.
26. Pyati, V. P. (1993). Computation of the circular error probability (CEP) integral. *IEEE Transactions on Aerospace and Electronic Systems, 29*(3), 1023-1024.
27. Shnidman, D. A. (1995). Efficient computation of the circular error probability (CEP) integral. *IEEE Transactions on Automatic Control, 40*(8), 1472-1474.
28. Ignagni, M. (2010). Determination of circular and spherical position-error bounds in system performance analysis. *Journal of Guidance, Control, and Dynamics, 33*(4), 1301-1305.
29. Krempasky, J. J. (2003). CEP equation exact to the fourth order. *Navigation, 50*(3), 143-149.
30. Abramowitz, M., & Stegun, I. A. (Eds.). (1968). *Handbook of mathematical functions with formulas, graphs, and mathematical tables* (Vol. 55). US Government printing office.
31. Huang, Y., Benesty, J., & Chen, J. (2006). Time delay estimation and acoustic source localization. *Acoustic MIMO signal processing*, 215-259.
32. Cheung, K. W., So, H. C., Ma, W. K., & Chan, Y. T. (2006). A constrained least squares approach to mobile positioning: algorithms and optimality. *EURASIP Journal on Advances in Signal Processing, 2006*, 1-23.
33. Chan, Y. T., & Ho, K. C. (1994). A simple and efficient estimator for hyperbolic location. *IEEE transactions on signal processing, 42*(8), 1905-1915.
34. Huang, Y., Benesty, J., Elko, G. W., & Mersereati, R. M. (2001). Real-time passive source localization: A practical linear-correction least-squares approach. *IEEE transactions on Speech and Audio Processing, 9*(8), 943-956.
35. Liu, H., Tang, Y., & Zhang, H. H. (2009). A new chi-square approximation to the distribution of non-negative definite quadratic forms in non-central normal variables. *Computational Statistics & Data Analysis, 53*(4), 853-856.

Appendix A. On Integration of $\widehat{J}_0^B$

Integral $\widehat{J}_0^B$ is equal to

$$\widehat{J}_0^B = \frac{1}{\sqrt{\lambda_1\lambda_2}}\int_0^B s\exp\left[-\left(\frac{1}{4\lambda_1}+\frac{1}{4\lambda_2}\right)s^2\right]\left[1+\sum_{k=1}^{M_0}\frac{\Omega^{2k}s^{4k}}{2^{3k-1}k!}\right]\mathrm{d}s = \frac{2\sqrt{\lambda_1\lambda_2}}{\lambda_1+\lambda_2}\left(1-\mathrm{e}^{-\frac{\rho}{2\gamma}}\right)+\sum_{k=1}^{M_0}\frac{\Omega^{2k}}{2^{3k-1}k!}J_k,$$

$$J_k = \frac{1}{\sqrt{\lambda_1\lambda_2}}\int_0^B s^{4k+1}\exp\left[-\left(\frac{1}{4\lambda_1}+\frac{1}{4\lambda_2}\right)s^2\right]\mathrm{d}s.$$

Applying to J_k the rule of by parts integration we obtain:

$$\upsilon^{-1}J_k = -\int_0^B s^{4k}\mathrm{d}\exp\left[-\left(\frac{1}{4\lambda_1}+\frac{1}{4\lambda_2}\right)s^2\right] = -s^{4k}\exp\left[-\left(\frac{1}{4\lambda_1}+\frac{1}{4\lambda_2}\right)s^2\right]\Bigg|_0^B + 4k\int_0^B s^{4k-1}\exp\left[-\left(\frac{1}{4\lambda_1}+\frac{1}{4\lambda_2}\right)s^2\right]\mathrm{d}s =$$

$$= 4k(4k-2)\ldots4\times2\gamma^{2k} - e^{-\frac{\rho}{2\gamma}}\left\{\rho^{2k}+4k\gamma\rho^{2k-1}+\ldots+4k(4k-2)\ldots4\times2\gamma^{2k}\right\},\ \upsilon = 2\sqrt{\lambda_1\lambda_2}\big/(\lambda_1+\lambda_2).$$

Appendix B. On Integration of $\widehat{J}_{R_\lambda}^{R99_A}$

Change of variable $s = u\big/\sqrt{2\lambda_1}$ in integral $\widehat{J}_{R_\lambda}^{R99_A}$ leads to

$$\widehat{J}_{R_\lambda}^{R99_A} = \frac{2}{\sqrt{\pi}}\sqrt{\frac{\lambda_1}{\lambda_1-\lambda_2}}\left\{\int_{\frac{R_\lambda}{\sqrt{2\lambda_1}}}^{\frac{R99_A}{\sqrt{2\lambda_1}}}\mathrm{e}^{-u^2}\mathrm{d}u + \sum_1^{M_\infty}\frac{\prod_{s=1}^{k}(2s-1)^2}{(16\lambda_1\Omega)^k k!}J_k^\infty\right\},\ J_k^\infty = \int_{\frac{R_\lambda}{\sqrt{2\lambda_1}}}^{\frac{R99_A}{\sqrt{2\lambda_1}}}\frac{\mathrm{e}^{-u^2}}{u^{2k}}\mathrm{d}u$$

Integral J_k^∞ is performed by parts:

$$J_k^\infty = \frac{-1}{(2k-1)}\int_{\frac{R_\lambda}{\sqrt{2\lambda_1}}}^{\frac{R99_A}{\sqrt{2\lambda_1}}}\mathrm{e}^{-u^2}\,\mathrm{d}\frac{1}{u^{2k-1}} = \frac{-1}{(2k-1)}\left(\frac{\mathrm{e}^{-u^2}}{u^{2k-1}}\Bigg|_{\frac{R_\lambda}{\sqrt{2\lambda_1}}}^{\frac{R99_A}{\sqrt{2\lambda_1}}} + 2\int_{\frac{R_\lambda}{\sqrt{2\lambda_1}}}^{\frac{R99_A}{\sqrt{2\lambda_1}}}\frac{\mathrm{e}^{-u^2}}{u^{2k-2}}\mathrm{d}u\right) =$$

$$= \frac{-1}{(2k-1)}\left(\frac{\mathrm{e}^{-u^2}}{u^{2k-1}}\Bigg|_{\frac{R_\lambda}{\sqrt{2\lambda_1}}}^{\frac{R99_A}{\sqrt{2\lambda_1}}} + \frac{-2}{(2k-3)}\left(\frac{\mathrm{e}^{-u^2}}{u^{2k-3}}\Bigg|_{\frac{R_\lambda}{\sqrt{2\lambda_1}}}^{\frac{R99_A}{\sqrt{2\lambda_1}}} + 2\int_{\frac{R_\lambda}{\sqrt{2\lambda_1}}}^{\frac{R99_A}{\sqrt{2\lambda_1}}}\frac{\mathrm{e}^{-u^2}}{u^{2k-4}}\mathrm{d}u\right)\right) =$$

$$= \frac{1}{(2k-1)}\left[\frac{e^{-\frac{R_\lambda^2}{2\lambda_1}}}{\left(\frac{R_\lambda}{\sqrt{2\lambda_1}}\right)^{2k-1}} - \frac{e^{-\frac{R99_A^2}{2\lambda_1}}}{\left(\frac{R99_A}{\sqrt{2\lambda_1}}\right)^{2k-1}}\right] - \frac{2}{(2k-1)(2k-3)}\left[\frac{e^{-\frac{R_\lambda^2}{2\lambda_1}}}{\left(\frac{R_\lambda}{\sqrt{2\lambda_1}}\right)^{2k-3}} - \frac{e^{-\frac{R99_A^2}{2\lambda_1}}}{\left(\frac{R99_A}{\sqrt{2\lambda_1}}\right)^{2k-3}}\right] +$$

$$+\frac{4}{(2k-1)(2k-3)(2k-5)}\left[\frac{e^{-\frac{R_\lambda^2}{2\lambda_1}}}{\left(\frac{R_\lambda}{\sqrt{2\lambda_1}}\right)^{2k-5}}-\frac{e^{-\frac{R99_A^2}{2\lambda_1}}}{\left(\frac{R99_A}{\sqrt{2\lambda_1}}\right)^{2k-5}}\right]-\ldots+\frac{(-2)^{\kappa-1}}{(2k-1)\ldots\times5\times3\times1}\left[\frac{e^{-\frac{R_\lambda^2}{2\lambda_1}}}{\left(\frac{R_\lambda}{\sqrt{2\lambda_1}}\right)}-\frac{e^{-\frac{R99_A^2}{2\lambda_1}}}{\left(\frac{R99_A}{\sqrt{2\lambda_1}}\right)}\right]+$$

$$+\frac{(-2)^{\kappa}}{(2k-1)\ldots\times5\times3\times1}\int_{\frac{R_\lambda}{\sqrt{2\lambda_1}}}^{\frac{R99_A}{\sqrt{2\lambda_1}}}\mathrm{e}^{-u^2}\,\mathrm{d}u=\frac{(-2)^{k}}{\prod_{s=1}^{k}\left[2(k-s)+1\right]}\int_{\frac{R_\lambda}{\sqrt{2\lambda_1}}}^{\frac{R99_A}{\sqrt{2\lambda_1}}}\mathrm{e}^{-u^2}\,\mathrm{d}u+$$

$$+\sum_{\ell=1}^{k}\frac{(-2)^{\ell-1}}{\prod_{s=1}^{\ell}\left[2(k-s)+1\right]}\left[\frac{e^{-\frac{R_\lambda^2}{2\lambda_1}}}{\left(\frac{R_\lambda}{\sqrt{2\lambda_1}}\right)^{2(k-\ell)+1}}-\frac{e^{-\frac{R99_A^2}{2\lambda_1}}}{\left(\frac{R99_A}{\sqrt{2\lambda_1}}\right)^{2(k-\ell)+1}}\right].$$